Princeton Plasma Physics Laboratory

PPPL-5329

Momentum Flux Parasitic to Free-Energy Transfer

T. Stoltzfus-Dueck

December 2016

PRINCETON PLASMA PHYSICS LABORATORY

Prepared for the U.S.Department of Energy under Contract DE-AC02-09CH11466.

Momentum flux parasitic to free-energy transfer

T Stoltzfus-Dueck[1] and B Scott[2]

[1]Princeton University, Princeton, NJ 08544
[2]Max-Planck-Institut für Plasmaphysik, Boltzmannstr. 2, D-85748 Garching, Germany

E-mail: `tstoltzf@princeton.edu`

Abstract. An often-neglected portion of the radial $\boldsymbol{E} \times \boldsymbol{B}$ drift is shown to drive an outward flux of co-current momentum when free energy is transferred from the electrostatic potential to ion parallel flows. This symmetry breaking is fully nonlinear, not quasilinear, necessitated simply by free-energy balance in parameter regimes for which significant energy is dissipated via ion parallel flows. The resulting rotation peaking has a scaling and order of magnitude that are comparable with experimental observations. The residual stress becomes inactive when frequencies are much higher than the ion transit frequency, which may explain the observed relation of density and counter-current rotation peaking in the core.

PACS numbers: 52.25.Dg, 52.25.Fi, 52.25.Xz, 52.30.Gz, 52.35.We, 52.55.Dy, 52.55.Fa

Keywords: toroidal rotation, tokamak, transport, intrinsic rotation, rotation reversal

Submitted to: *Nucl. Fusion*

1. Introduction

Axisymmetric laboratory plasmas routinely exhibit nonzero, sheared toroidal rotation in the absence of applied torque [1], beneficial for fusion since toroidal rotation suppresses resistive wall modes [2]. This so-called intrinsic rotation may play an important role in determining the performance of ITER and of any future burning plasma device, since these devices will be able to apply only comparatively weak external torque [3].

The toroidal rotation profiles of tokamak discharges without applied torque typically display three distinct radial regions [4, 5, 6, 7, 8, 9, 10]. The steep-gradient edge region, from the pedestal top and outwards in H-mode, usually rotates in the co-current direction due to the interaction of ion orbit shifts and spatial variation of the turbulent fluctuation amplitude [10, 11, 12, 13]. Rotation in the mid-radius "gradient" region, extending from the sawtooth inversion radius out to the pedestal top, is often more counter-current at its inner radial edge than its outer edge ("counter-current peaking"), but may also exhibit a flat rotation profile ("rotation reversal"), and can switch rapidly between these two states as plasma parameters (such as plasma current I_p or density) cross threshold values [6, 8, 14, 15]. The innermost ("sawtoothing") region, inside the $q = 1$ surface, has a rotation profile that is strongly affected by sawtooth crashes, typically flat or weakly co-current peaked. The present work focuses on the enigmatic behavior in the mid-radius gradient region.

Intrinsic rotation in the mid-radius region has already been extensively studied, both experimentally and theoretically [1, 16]. Nonaxisymmetric equilibrium magnetic geometry can strongly affect rotation [17]. For an axisymmetric geometry, as we assume for the entirety of this article, toroidal angular momentum conservation [18, 19] implies that peaking without applied torque must follow from a nondiffusive momentum flux. Since neoclassical (collisional) momentum fluxes are much too small to explain experimental observations [1, 20], we will focus on turbulent momentum flux. Although theoretical mechanisms for momentum pinches (momentum flux terms proportional to the rotation itself rather than its radial gradient) have been identified [21, 22], they cannot explain the common observation of peaked rotation profiles passing through zero rotation [4, 5, 6, 7, 8, 9, 10]. Accordingly, most present models focus on residual stress (momentum flux terms independent of both the rotation and the rotation gradient), which however are restricted for delta-f calculations in an up-down symmetric magnetic geometry [16]. The present work offers a new symmetry-breaking residual stress mechanism, due to $\boldsymbol{E}\times\boldsymbol{B}$ advection of parallel toroidal angular momentum by a portion of the $\boldsymbol{E}\times\boldsymbol{B}$ drift that is neglected in most delta-f models.

For a simple physical picture, consider a low-frequency axisymmetric density perturbation, as sketched in Fig. 1. At low frequencies and large scales, the nonzonal electrostatic potential $\tilde{\phi}$ is proportional to the nonzonal electron density $\tilde{n}_e$, which approximately equals ion charge state Z times nonzonal ion gyrocenter density $\tilde{n}_i$. The parallel components of the ion pressure gradient and electric field jointly cause ion flow out of the dense region along the magnetic field. The poloidal electric field also causes an $\boldsymbol{E}\times\boldsymbol{B}$ drift $\boldsymbol{v}_E$ that advects counter- (co-)current ion momentum radially inward (outward), regardless of the plasma's toroidal rotation, its radial gradient, and the signs of the plasma current I_p and toroidal magnetic field B_T. Although very simple, this basic spin-up mechanism can occur in many contexts, and is in fact a necessary consequence of damping via parallel ion flow in toroidal geometry.

The symmetry breaking underlying this spin-up mechanism is due to a dual role for the electric field caused by the weak poloidal variation of $\tilde{\phi}$ on the length scale of the minor radius r. FIRST ROLE: The nonvanishing parallel projection of this electric field locally causes ion parallel acceleration. This acceleration mediates a free energy transfer from the potential to the ion parallel flows. Since the free energy source terms for the turbulence supply energy predominantly to the even moments of the distribution function (like density and pressure) while much of the dissipation acts on odd moments of the distribution function, steady-state energy balance demands a net free-energy transfer from even to odd moments. For fluctuations at frequency scales comparable to the ion transit frequency, this transfer mostly occurs via the ion parallel acceleration, implying a positive correlation between the parallel electric field and parallel ion flow. SECOND ROLE: Now consider the contribution of the electric field to the toroidal angular momentum equation. Conservation of toroidal angular momentum implies that this self-generated electric field may not cause a net toroidal acceleration

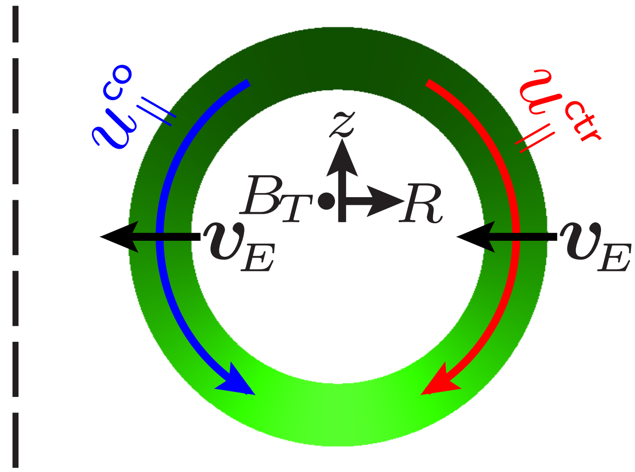

Figure 1. Poloidal cross-section of low-frequency axisymmetric fluctuations, indicating direction of increasing major radius R and vertical position z. Darker shading shows larger $\tilde{n}_i$, proportional to $\tilde{\phi}$ by the low-$k_\perp$ electron adiabatic response. With time, ions flow along the magnetic field out of the dense region, corresponding to counter-current toroidal flow (red, $u_\parallel^{\rm ctr}$) toward decreasing θ and co-current (blue, $u_\parallel^{\rm co}$) toward increasing θ. The poloidal variation of $\tilde{\phi}$ also causes an $\boldsymbol{E}\times\boldsymbol{B}$ flow $\boldsymbol{v}_E$ that is radially inward for the counter-current ion flux and outward for the co-current flux. Reversing the toroidal magnetic field switches the poloidal direction of counter- and co-current flow as well as the sign of $\boldsymbol{v}_E$, leaving the momentum flux unchanged. The poloidal orientation of the density perturbation has no effect on the sign or magnitude of this momentum flux.

of the plasma. However, the slow poloidal variation of $\tilde{\phi}$ may cause a weak radial $\boldsymbol{E}\times\boldsymbol{B}$ drift, transporting angular momentum inwards or outwards. The positive correlation of parallel electric field and ion parallel flows, due to steady-state free energy balance, implies a positive correlation of co-current toroidal flow and outward $\boldsymbol{E}\times\boldsymbol{B}$ drift, as sketched in Fig. 1. This is the fundamental symmetry-breaking mechanism underlying the spin-up discussed in this article.

As one example, such a momentum flux is caused by ion Landau damping of GAMs, as derived in Ref. [23]: First, turbulent Reynolds stress excites a poloidal $\boldsymbol{E}\times\boldsymbol{B}$ flow. Due to poloidal variation of B, this flow has a divergence that leads to an up/down density asymmetry, as sketched in Fig. 1. The resulting parallel electric field (due to electron adiabatic response) and ion pressure gradient drive parallel ion flows. When the GAM is ion Landau damped, there is net energy transfer from the fluctuating potential to the parallel ion flows, which implies a positive correlation of the poloidal electric field with the poloidal ion flow. This same poloidal electric field causes a weak radial $\boldsymbol{E}\times\boldsymbol{B}$ drift, which is also correlated with ion parallel flow. Due to the pitch of the magnetic field, the parallel ion flow corresponds to co- (counter-)current toroidal flow where the $\boldsymbol{E}\times\boldsymbol{B}$ drift points radially outward (inward), which causes counter-current rotation peaking. Interestingly, it is the *poloidal* flows driven by the Reynolds stress that lead to the density fluctuations and the ion Landau damping, which then as a byproduct result in the nondiffusive transport of *toroidal* momentum. For strongly ion-Landau-damped GAMs, this mechanism should drive intrinsic toroidal ion thermal Mach numbers of order (ρ_i/r). Even stronger spin-up may occur due to ion Landau damping of nonaxisymmetric turbulent fluctuations. In this article, we investigate both the axisymmetric and nonaxisymmetric flow drive, using a conservative gyrokinetic formulation.

The rest of the article is organized as follows: In Sec. 2, we will present the gyrokinetic models underlying our analysis, both a momentum- and energy-conserving full-F formulation (Sec. 2.1, with detailed derivations deferred to Appendix A and Appendix B) and a free-energy-conserving delta-f formulation (Secs. 2.2 and 2.3). In Sec. 3 we discuss restrictions on the lowest-order residual stress in our delta-f model, assuming up-down symmetric magnetic geometry. Sec. 4 derives the momentum flux contribution due to a geometrically subdominant portion of the $\boldsymbol{E}\times\boldsymbol{B}$ drift, then demonstrates that it is not only *allowed* to cause residual stress, but in fact *required* to do so by free-energy balance whenever $\tilde{\phi}$ excites ion parallel flows. Sec. 5 discusses the results, and Sec. 6 summarizes our conclusions.

2. Gyrokinetic Models and Conservation Properties

Analysis will rest on a self-consistent, conservative electromagnetic gyrokinetic formulation derived using Lagrangian field theory, following Refs. [24] and [25]. To allow multiple viewpoints on the physics, we will employ both a radially global full-F formulation and a radially local delta-f formulation. These models and their basic conservation properties are respectively presented in Secs. 2.1 and 2.2, with an even/odd delta-f decomposition given in Sec. 2.3. For a simpler but roughly equivalent isothermal gyrofluid formulation, see Ref. [23].

2.1. Full-F, radially global

In the full-F model, derived in Appendix A, we evolve the full gyrokinetic distribution function F_s for each species s in a radially global geometry. For pedagogical reasons, we use a symplectic representation, with magnetic fluctuations captured by the contribution of the fluctuating parallel component of the vector potential $A_\parallel$ to the generalized $\boldsymbol{A}^* \doteq \boldsymbol{A} + (J_0 A_\parallel + \frac{c}{Ze} m_s v_\parallel)\hat{\boldsymbol{b}}$, with $\nabla\times\boldsymbol{A}=\boldsymbol{B}$ the equilibrium magnetic field, J_0 the gyroaveraging operator [assumed to be independent of $v_\parallel$, t, and simple toroidal angle φ, and to be self-adjoint under volume integration], $\hat{\boldsymbol{b}} \doteq \boldsymbol{B}/B$ the equilibrium magnetic direction, e the (positive) fundamental charge, and Z and m_s the species charge state (-1 for electrons) and mass.

The gyrocenter position $\boldsymbol{R}$ and parallel velocity $v_\parallel$ evolve according to

$$B_\parallel^* \dot{\boldsymbol{R}} = \frac{c}{Ze}\hat{\boldsymbol{b}} \times \nabla H + v_\parallel \boldsymbol{B}^*, \tag{1}$$

$$B_\parallel^* m_s \dot{v}_\parallel = -\boldsymbol{B}^* \cdot \nabla H - B_\parallel^* \frac{Ze}{c}\partial_t J_0 A_\parallel, \tag{2}$$

with $\boldsymbol{B}^* \doteq \nabla \times \boldsymbol{A}^*$ and $B_\parallel^* \doteq \hat{\boldsymbol{b}} \cdot \boldsymbol{B}^*$. The Hamiltonian H is decomposed by powers of the electrostatic potential ϕ: $H = H_0 + H_1 + H_p$ with $H_0 = \frac{1}{2}m_s v_\parallel^2 + \mu B$, $H_1 = ZeJ_0\phi$, and polarization contribution $H_p = -\frac{Z^2e^2}{2B}\partial_\mu[J_0(\phi^2) - (J_0\phi)^2]$. The magnetic moment is conserved: $\dot{\mu} = 0$.

The distribution function $F_s(\boldsymbol{R}, v_\parallel, \mu, t)$ evolves as

$$\partial_t(B_\parallel^* F_s) + \nabla \cdot (B_\parallel^* F_s \dot{\boldsymbol{R}}) + \partial_{v_\parallel}(B_\parallel^* F_s \dot{v}_\parallel) = 0. \tag{3}$$

The time-dependent Liouville theorem,[1]

$$\partial_t B_\parallel^* + \nabla \cdot (B_\parallel^* \dot{\boldsymbol{R}}) + \partial_{v_\parallel}(B_\parallel^* \dot{v}_\parallel) = 0, \tag{4}$$

allows us to use an equivalent advection form:

$$d_t F_s \doteq \partial_t F_s + \dot{\boldsymbol{R}} \cdot \nabla F_s + \dot{v}_\parallel \partial_{v_\parallel} F_s = 0. \tag{5}$$

The field equations, self-consistently determined from the same Lagrangian, are the quasineutrality relation for ϕ,

$$\sum_s \int \frac{\mathrm{d}\mathcal{W}}{B_\parallel^*}\Big[ZeJ_0(B_\parallel^* F_s) + J_0(B_\parallel^* \mathcal{M} J_0\phi) - \phi J_0(B_\parallel^* \mathcal{M})\Big] = 0, \tag{6}$$

with polarizability

$$\mathcal{M} \doteq -\frac{Z^2e^2}{BB_\parallel^*}\partial_\mu(B_\parallel^* F_s), \tag{7}$$

and a gyrokinetic Ampère's Law,

$$\nabla_\perp^2 A_\parallel = -\frac{4\pi}{c}\sum_s \int \frac{\mathrm{d}\mathcal{W}}{B_\parallel^*} ZeJ_0(B_\parallel^* v_\parallel F_s), \tag{8}$$

with $\sum_s$ the sum over species, $\nabla_\perp^2$ the divergence of the perpendicular gradient $\nabla_\perp$, and $\int \mathrm{d}\mathcal{W} \doteq (2\pi/m_s)\int_0^\infty \mathrm{d}\mu \int_{-\infty}^\infty \mathrm{d}v_\parallel\, B_\parallel^*$ indicating integration over velocity space. With this definition, $\int \mathrm{d}\mathcal{W}/B_\parallel^*$ commutes with spatial differentiation and integration and annihilates velocity-space derivatives. We indicate real-space volume integration with $\int \mathrm{d}\mathcal{V}$ and integration over all of phase space with $\int \mathrm{d}\Lambda \doteq \int \mathrm{d}\mathcal{V} \int \mathrm{d}\mathcal{W}$. Using the enclosed volume V as a flux surface label and denoting an integral over the volume inside the corresponding flux surface with $\int_V \mathrm{d}\mathcal{V}$, we may define the flux surface average $\langle\cdots\rangle \doteq \partial_V \int_V \mathrm{d}\mathcal{V} \sum_s \int \mathrm{d}\mathcal{W}$ for kinetic functions like F_s and $\langle\cdots\rangle \doteq \partial_V \int_V \mathrm{d}\mathcal{V}$ for purely spatial functions like ϕ [18, 26].

The gyrokinetic system of equations [Eqs. (1)–(3) and (6)–(8)] conserve a total energy $(\sum_s U_s) + U_E + U_M$ with thermal energies $U_s \doteq \int \mathrm{d}\Lambda\, H_0 F_s$, $\boldsymbol{E} \times \boldsymbol{B}$ energy $U_E \doteq \sum_s \int \mathrm{d}\Lambda\, \frac{1}{2}\mathcal{M}[J_0(\phi^2) - (J_0\phi)^2]$, and magnetic fluctuation energy $U_M \doteq \frac{1}{8\pi}\int \mathrm{d}\mathcal{V}\, |\nabla_\perp A_\parallel|^2$. Assuming boundary terms to vanish, the separate components evolve as[2]

$$\partial_t U_s = -\int \mathrm{d}\Lambda\, F_s\Big[\dot{\boldsymbol{R}} \cdot \nabla(H_1 + H_p) + \frac{Ze}{c}v_\parallel \partial_t J_0 A_\parallel\Big], \tag{9}$$

$$\partial_t U_E = \sum_s \int \mathrm{d}\Lambda\, F_s \dot{\boldsymbol{R}} \cdot \nabla(H_1 + H_p), \tag{10}$$

$$\partial_t U_M = \sum_s \int \mathrm{d}\Lambda\, F_s \frac{Ze}{c} v_\parallel \partial_t J_0 A_\parallel, \tag{11}$$

showing particle-field energy exchange due to flow up and down the electrostatic potential energy $(H_1 + H_p)$ and the inductive parallel electric field $-\frac{1}{c}\partial_t J_0 A_\parallel$. Due to the symplectic formulation used here, toroidal angular momentum conservation takes a slightly different form than in Ref. [18] (see Appendix B):

$$\begin{aligned}\partial_t\big\langle F_s(m_s v_\parallel + ZeJ_0A_\parallel/c)b_\varphi\big\rangle - \partial_t\left\langle \boldsymbol{P} \cdot \nabla A_\varphi\right\rangle/c \\ = -\partial_V\left\langle F_s(m_s v_\parallel + ZeJ_0A_\parallel/c)b_\varphi \dot{\boldsymbol{R}} \cdot \nabla V\right\rangle \\ -\big\langle F_s \partial_\varphi\left(H - Zev_\parallel J_0 A_\parallel/c\right)\big\rangle,\end{aligned} \tag{12}$$

in which $b_\varphi \doteq \hat{\boldsymbol{b}} \cdot R^2\nabla\varphi$, $A_\varphi \doteq \boldsymbol{A} \cdot R^2\nabla\varphi$, and $\partial_\varphi \doteq [(R^2\nabla\varphi) \cdot \nabla]$, for simple toroidal angle φ and major radius R. The terms on the LHS respectively show the forms for the parallel and $\boldsymbol{E}\times\boldsymbol{B}$ contributions to the toroidal angular momentum, the latter expressed in terms of the polarization vector $\boldsymbol{P}$, defined by Eq. (B.5). The terms on the RHS give the divergence of the radial fluxes of the parallel and $\boldsymbol{E}\times\boldsymbol{B}$ portions[3] of the toroidal angular momentum. Appendix B also demonstrates that the final term is indeed the divergence of a radial flux.

As derived in Appendix A, one may simplify the above formulation by linearizing the polarization contribution. To do this, one need only simplify the Hamiltonian to $H_0 + H_1$ (i.e. neglect H_p) and make the substitution $\mathcal{M} \to \mathcal{M}_M$ in Eq. (6), where $\mathcal{M}_M$ is defined in Eq. (A.11). The simplified system still conserves energy as in Eqs. (9)–(11) with the substitutions $(H_1 + H_p) \to H_1$ in Eqs. (9) and (10) and $\mathcal{M} \to \mathcal{M}_M$ in the definition of U_E. The simplified system also still conserves toroidal

[1] Note that $v_\parallel$ is an independent variable in this formulation, so for example $\nabla v_\parallel = 0$ and $\partial_{v_\parallel}\nabla H = 0$.

[2] Act on Eq. (3) with $\int(\mathrm{d}\Lambda/B_\parallel^*)H_0$, on Eq. (6) with $\int \mathrm{d}\mathcal{V}\,\phi\partial_t$, and on Eq. (8) with $-(4\pi)^{-1}\int \mathrm{d}\mathcal{V}\,(\partial_t A_\parallel)$. Use the facts that J_0 is independent of t and $v_\parallel$, that J_0 is self-adjoint under $\int \mathrm{d}\mathcal{V}$, and that J_0 becomes the identity at $\mu = 0$. For U_E, separate the terms $\partial_t U_E$ and $\sum_s \int(\mathrm{d}\Lambda/B_\parallel^*)(H_1 + H_p)\partial_t(B_\parallel^* F_s)$, then substitute for $\partial_t(B_\parallel^* F_s)$ using Eq. (3).

[3] The two portions of the final term correspond to Reynolds and Maxwell stresses, respectively.

angular momentum as in Eq. (12), interpreted with the simplified Hamiltonian. We will use linearized polarization for the derivation of the delta-f model in Sec. 2.2.

2.2. Delta-f, radially local

Since the literature contains multiple distinct definitions for the delta-f model, we begin this section by clarifying the approximations going into our delta-f formulation for this article. Our approach closely follows Ref. [25], but is not identical.[4] We will decompose the total distribution function as $F_s = F_{sM} + f_s$, with static, spatially slowly varying background portion F_{sM} and time-dependent, small-amplitude portion f_s. We consider small-scale, anisotropic turbulence, with parallel wavelengths on the macroscopic scale ($k_\parallel \sim 1/qR$) but characteristic perpendicular wavenumbers $k_\perp$ satisfying $\rho_i \lesssim k_\perp^{-1} \ll L_\perp \lesssim r, R$ for $\rho_s \doteq v_{ts}/|\Omega_{cs}|$ the species (thermal) gyroradius, $v_{ts} \doteq (T_{s0}/m_s)^{1/2}$ the species thermal speed, Ω_{cs} the (signed) species gyrofrequency, and $L_\perp$ the length scale of profile gradients. The fluctuating distribution function is mixing-length-ordered ($k_\perp f_s \sim F_{sM}/L_\perp$) and the magnetic fluctuations are taken small ($k_\perp A_\parallel/B \ll 1$). We will cast the equation in a radially local geometry, neglecting radial variation of background parameters outside of explicit gradient terms (∼the 'constant-F_{sM}, constant-grad-F_{sM}' approximation). Due to careful construction of the local geometry, we will be able to straightforwardly demonstrate the conservation of a 'free energy,' quadratic in the fluctuations and related to entropy, that measures the amplitude of the turbulence and exposes transfer mechanisms between f_s, ϕ, and $A_\parallel$. Higher-order corrections to f_s are not necessary here, since the leading-order fluctuations will uniquely determine the contribution of our residual-stress mechanism.

We begin with the linearized-polarization version of Eq. (5), multiplied by $B^*_\parallel$. Expanding $F_s \to F_{sM}+f_s$ and discarding several unambiguously small terms, we obtain

$$B\partial_t f_s + \left(\frac{c}{Ze}\hat{\boldsymbol{b}}\times\nabla H + v_\parallel \boldsymbol{B}^*\right)\cdot\nabla(F_{sM}+f_s) - \frac{\boldsymbol{B}\cdot\nabla H_0}{m_s}\partial_{v_\parallel} f_s = m_s^{-1}\big(\boldsymbol{B}^*\cdot\nabla H + B(Ze/c)\partial_t J_0 A_\parallel\big)\partial_{v_\parallel} F_{sM}, \quad (13)$$

in which $H = H_0 + H_1$. We assume a nonrotating Maxwellian background $F_{sM} = n_{s0}(2\pi T_{s0}/m_s)^{-3/2}\exp(-H_0/T_{s0})$, in which the background density n_{s0} and (isotropic) temperature T_{s0} are flux functions. Since spatial derivatives are taken at constant μ, the gradient of F_{sM} decomposes as $\nabla F_{sM} = (\partial_V|_B F_{sM})\nabla V + (\partial_B|_V F_{sM})\nabla B$, where $(\partial_V F_{sM})$ brings in the profile gradients and $(\partial_B F_{sM})$ yields the zeroth-order relation $m_s v_\parallel(\partial_B F_{sM})\nabla B = (\partial_{v_\parallel} F_{sM})\nabla H_0$, which we use repeatedly in this section.

Under our assumptions and taking the background to be charge neutral ($\sum_s Zen_{s0} = 0$), the linearized-polarization Poisson equation and the Ampere's Law simplify to[5,6]

$$0 = \sum_s \int \mathrm{d}\mathcal{W}\left[ZeJ_0 f_s + (Z^2e^2/T_{s0})F_{sM}(J_0^2-1)\phi\right], \quad (14)$$

$$\nabla_\perp^2 A_\parallel = -\frac{4\pi}{c}\sum_s \int \mathrm{d}\mathcal{W}\, Zev_\parallel J_0 f_s, \quad (15)$$

in which the velocity-space integral is simplified to its delta-f form $\int \mathrm{d}\mathcal{W} \doteq (2\pi B/m_s)\int_0^\infty \mathrm{d}\mu \int_{-\infty}^\infty \mathrm{d}v_\parallel$.

Now we must construct the simplified geometry, starting with local coordinates that expose the symmetry properties of this delta-f system. We begin with unit-Jacobian Hamada coordinates: enclosed volume (flux label) V and unit-periodic poloidal (θ) and toroidal (ζ) angles, defined such that the contravariant components of $\boldsymbol{B}$ are flux functions, $B^\theta \doteq \boldsymbol{B}\cdot\nabla\theta = B^\theta(V)$ and $B^\zeta = \boldsymbol{B}\cdot\nabla\zeta = B^\zeta(V)$ [26, 27, 28]. Both V and θ are axisymmetric, while ζ equals an axisymmetric function plus $\varphi/2\pi$. The safety factor $q = B^\zeta/B^\theta$ is a flux function and the spatial Jacobian is unity, $(\nabla V\times\nabla\theta\cdot\nabla\zeta)^{-1} = 1$. Next, we define the field-aligned coordinates $\vartheta \doteq \theta$ and $\xi \doteq \zeta - q\theta$, which retain the unit Jacobian $(\nabla V\times\nabla\vartheta\cdot\nabla\xi)^{-1} = 1$ and satisfy $\boldsymbol{B} = B^\theta\nabla\xi\times\nabla V$, so that $\boldsymbol{B}\cdot\nabla = B^\theta\partial_\vartheta|_{V,\xi}$. Since V and ϑ are both axisymmetric, differentiating with respect to ξ brings in only toroidal variation, $\partial_\xi|_{V,\vartheta} = 2\pi R^2\nabla\varphi\cdot\nabla$, so the ξ partial vanishes for axisymmetric quantities. Finally, we scale with reference values to obtain local, length-dimensioned coordinates: $x \doteq (V-V_0)/V'$, $y \doteq -\xi V'/L_\parallel$, and $s \doteq \vartheta L_\parallel$, which satisfy $(\nabla x\times\nabla y\cdot\nabla s)^{-1} = 1$. The reference constants [connection length $L_\parallel \doteq B_0/B^\theta \sim 2\pi qR$, field strength B_0, enclosed volume V_0, and surface area V'] are all evaluated at a reference surface. Since $\partial_s \propto \boldsymbol{B}\cdot\nabla$, variation in s is weak even for turbulent quantities, $\partial_s = (\partial_s\vartheta)\partial_\vartheta \sim (L_\parallel^{-1})(Bk_\parallel/B^\theta) \sim k_\parallel \sim 1/qR$. The other derivatives capture perpendicular variation, with $\partial_x, \partial_y \sim k_\perp$ for turbulent/nonaxisymmetric quantities. [The combination $V'/L_\parallel \sim (2\pi r 2\pi R)/2\pi qR \sim 2\pi R(B_p/B_T)$, for B_p and B_T the poloidal and toroidal magnetic field strength, compensates for the fact

[4] In particular, Ref. [25] incorporated the profile gradients via boundary conditions on f_s, but in this work we will capture them in explicit volumetric terms.

[5] Note that the electromagnetic correction to $B^*_\parallel$ is two orders smaller than B, since $\hat{\boldsymbol{b}}\cdot\nabla(J_0A_\parallel)\times\hat{\boldsymbol{b}} = 0$. Also, $(1-J_0) \sim \rho_s^2/L_\perp^2$ is a second-order correction when it acts on slowly varying quantities, due to the low-$k_\perp$ expansion $J_0 \approx 1 + \frac{1}{4}\rho_s^2\nabla_\perp^2$. Note also that $(B^*_\parallel\mathcal{M}_M)$ is axisymmetric and slowly varying in space.

[6] For the Ampère's Law, we have removed the time-independent, axisymmetric current due to $(B^*_{\parallel M} - B)F_{sM}$. The corresponding magnetic field is incorporated into the external magnetic field, shifting it with finite-β adjustments relative to the external field used in the full-F formulation.

that $\partial_y \propto \nabla\varphi\cdot\nabla$ is nearly aligned with $\boldsymbol{B}\cdot\nabla$, leading to the simple ordering $\partial_y = (-L_\parallel/V')\partial_\xi|_{V,\vartheta} = (-L_\parallel/V')2\pi R^2\nabla\varphi\cdot\nabla \sim (B/2\pi RB_p)2\pi R(k_\perp B_p/B) = k_\perp$.] Although B_0, V_0, and V' are all positive, the constant $L_\parallel$ has the sign of B^θ, implying that the poloidal coordinate s is oriented such that $\boldsymbol{B}\cdot\nabla s > 0$.

Next, we evaluate our operators in the radially local geometry, assuming a radial domain width Δ much smaller than the profile gradient length $L_\perp$. The (linear) parallel gradient exactly satisfies $B\nabla_\parallel \doteq \boldsymbol{B}\cdot\nabla = B_0\partial_s$, with B the local magnetic field strength. Neglecting corrections of order $1/k_\perp r$ and using the Clebsch form $\boldsymbol{B} = B_0\nabla x\times\nabla y$, nonlinear $\boldsymbol{E}\times\boldsymbol{B}$ advection simplifies to

$$\frac{c\hat{\boldsymbol{b}}}{B}\times\nabla(J_0\phi)\cdot\nabla f_s = \frac{c\boldsymbol{B}}{B^2}\cdot\nabla(J_0\phi)\times\nabla f_s \approx \frac{c}{B_0}\{J_0\phi, f_s\}, \quad (16)$$

with the Poisson bracket defined e.g. as

$$\{J_0\phi, f_s\} \doteq (\partial_x J_0\phi)(\partial_y f_s) - (\partial_y J_0\phi)(\partial_x f_s). \quad (17)$$

The magnetic flutter takes an analogous Poisson bracket form, for example $B^{-1}v_\parallel\nabla\times(J_0A_\parallel\hat{\boldsymbol{b}})\cdot\nabla f_s \approx -B^{-1}v_\parallel\hat{\boldsymbol{b}}\times\nabla(J_0A_\parallel)\cdot\nabla f_s \approx -B_0^{-1}v_\parallel\{J_0A_\parallel, f_s\}$. Again neglecting $O(1/k_\perp r)$ corrections, the perpendicular Laplacian simplifies to $\nabla_\perp^2 \approx g^{xx}\partial_{xx}^2 + 2g^{xy}\partial_{xy}^2 + g^{yy}\partial_{yy}^2$, for $g^{xx} \doteq |\nabla x|^2$, $g^{xy} \doteq \nabla x\cdot\nabla y$, and $g^{yy} \doteq |\nabla y|^2$. We make the low-$\beta$ approximation $(\nabla\times\hat{\boldsymbol{b}})_\perp \approx \hat{\boldsymbol{b}}\times\nabla\ln B$,[7] after which the contributions of magnetic inhomogeneity [neglecting $O(1/k_\perp r)$ corrections] may be expressed in terms of a curvature operator $\mathcal{K}(\cdot) \doteq \mathcal{K}^x\partial_x + \mathcal{K}^y\partial_y$, with $\mathcal{K}^x \doteq -\frac{2c}{B}\hat{\boldsymbol{b}}\times\nabla\ln B\cdot\nabla x$ and $\mathcal{K}^y \doteq -\frac{2c}{B}\hat{\boldsymbol{b}}\times\nabla\ln B\cdot\nabla y$. Our geometry is then captured by six spatial functions: B, $\mathcal{K}^x$, $\mathcal{K}^y$, g^{xx}, g^{xy}, and g^{yy}. By axisymmetry of the geometry, these functions are (exactly) independent of y. Since we assume a narrow radial box width ($\Delta \ll L_\perp, R$), we may neglect their radial (x) variation as well, so each of the six functions are taken to depend on s alone. Further, after expanding $\nabla F_{sM} = F'_{sM}\nabla x + (-\mu F_{sM}/T_{s0})\nabla B$ for $F'_{sM} \doteq \partial_x|_B F_{sM}$, we neglect radial ($x$) variation of F_{sM} and F'_{sM}, corrections of order $\Delta/L_\perp$.

[7] Note first that $(\nabla\times\hat{\boldsymbol{b}})_\perp$ agrees with the standard form appearing in the curvature drift. Since $\hat{\boldsymbol{b}}\cdot\hat{\boldsymbol{b}} = 1$ is a constant, one may infer $(\hat{\boldsymbol{b}}\cdot\nabla)\hat{\boldsymbol{b}} = -\hat{\boldsymbol{b}}\times(\nabla\times\hat{\boldsymbol{b}})$, thus

$$\hat{\boldsymbol{b}}\times[(\hat{\boldsymbol{b}}\cdot\nabla)\hat{\boldsymbol{b}}] = -\hat{\boldsymbol{b}}\times[\hat{\boldsymbol{b}}\times(\nabla\times\hat{\boldsymbol{b}})] = (\nabla\times\hat{\boldsymbol{b}})_\perp.$$

Now, expand $(\nabla\times\hat{\boldsymbol{b}})$ using Ampere's Law:

$$\nabla\times\hat{\boldsymbol{b}} = \nabla\times(\boldsymbol{B}/B) = \hat{\boldsymbol{b}}\times\nabla\ln B + B^{-1}(4\pi/c)\boldsymbol{j}.$$

To compare the magnitudes of the perpendicular portions, take the ratio of $-\hat{\boldsymbol{b}}\times$ the two terms and use leading-order force balance $\frac{1}{c}\boldsymbol{j}\times\boldsymbol{B}\approx\nabla p$:

$$\frac{-\hat{\boldsymbol{b}}\times(4\pi/cB)\boldsymbol{j}}{-\hat{\boldsymbol{b}}\times\left(\hat{\boldsymbol{b}}\times\nabla\ln B\right)} \approx \frac{(4\pi/B^2)\nabla p}{\nabla_\perp\ln B} \sim \frac{4\pi p}{B^2}\frac{R}{L_\perp} = \frac{1}{2}\beta\frac{R}{L_\perp}.$$

With these approximations, Eq. (13) simplifies to the explicit form[8]

$$\begin{aligned}\partial_t f_s &+ \frac{Ze}{c}\frac{v_\parallel}{T_{s0}}F_{sM}\partial_t J_0A_\parallel + \frac{c}{B_0}\{J_0\psi_e, h_s\} + v_\parallel\nabla_\parallel h_s \\ &- \frac{1}{m_s}(\mu\nabla_\parallel B)\partial_{v_\parallel}h_s - \frac{1}{2Ze}(m_sv_\parallel^2+\mu B)\mathcal{K}(h_s) \\ &= \Big[\frac{c}{B_0}\partial_y(J_0\psi_e) + \frac{1}{2Ze}(\mu B + m_sv_\parallel^2)\mathcal{K}^x\Big]F'_{sM}, \quad (18)\end{aligned}$$

in which the nonadiabatic distribution function h_s and gyrokinetic potential ψ_e are defined as

$$h_s \doteq f_s + (F_{sM}/T_{s0})ZeJ_0\phi, \quad (19)$$

$$\psi_e \doteq \phi - v_\parallel A_\parallel/c. \quad (20)$$

The Poisson equation and Ampère's Law are formally unchanged from Eqs. (14) and (15), but are evaluated in the simplified geometry, that is, with the simplified form for $\nabla_\perp^2$ and taking F_{sM} and J_0 to depend spatially only on s. We may integrate J_0^2 over the Maxwellian in Eq. (14) to get the equivalent

$$\sum_s\int \mathrm{d}\mathcal{W}\, ZeJ_0f_s = \sum_s n_{s0}Z^2e^2\frac{1-\Gamma_{0s}}{T_{s0}}\phi, \quad (21)$$

in which the modified Bessel operator Γ_{0s} takes the Fourier-space form $\Gamma_{0s}(k_\perp^2\rho_s^2) = \exp(-k_\perp^2\rho_s^2)I_0(k_\perp^2\rho_s^2)$.[9] Eqs. (14) [or (21)], (15), and (18) constitute our delta-f gyrokinetic model.

The boundary conditions in y and s follow directly from toroidal and poloidal periodicity [28]. In the original Hamada coordinates, toroidal and poloidal periodicity are $f_s(V,\theta,\zeta=1/2) = f_s(V,\theta,\zeta=-1/2)$ and $f_s(V,\theta=1/2,\zeta) = f_s(V,\theta=-1/2,\zeta)$, where we centered the domain on $\theta = 0$ and $\zeta = 0$ for definiteness. In the field-aligned coordinates, advancing ξ by one (at fixed V and ϑ) is equivalent to advancing ζ by one (at fixed V and θ), so we maintain simple periodicity in ξ: $f_s(V,\vartheta,\xi=1/2) = f_s(V,\vartheta,\xi=-1/2)$. However, advancing θ by one

[8] In Eq. (18), we have also simplified with the zeroth-order relation $m_sv_\parallel(\partial_BF_{sM})\nabla B = (\partial_{v_\parallel}F_{sM})\nabla H_0$ (first dotted with $\boldsymbol{B}^*$, then later again, dotted with $H_1\boldsymbol{B}$), the antisymmetry of the Poisson bracket, and the fact that F_{sM} is independent of x and y.

[9] For example, one may integrate the operator's series expansion, term by term. The Bessel operator J_0 takes the Fourier-space form $J_0(k_\perp\rho)$, where $\rho^2 = 2\mu B/m_s\Omega_{cs}^2$. Mapping $k_\perp^2 \to -\nabla_\perp^2$, we may use the Taylor expansion of J_0^2 to define the operator as a series, $J_0^2 = \sum_{\ell=0}^\infty[(2\ell)!/(\ell!)^4](\rho^2/4)^\ell\nabla_\perp^{2\ell}$. We may then use the fact that $\int\mathrm{d}\mathcal{W}\,\mu^\ell F_{sM} = n_{s0}(\ell!)(T_{s0}/B)^\ell$ to integrate term by term:

$$\begin{aligned}\int\mathrm{d}\mathcal{W}F_{sM}J_0^2\phi &= \sum_{\ell=0}^\infty\frac{(2\ell)!}{(\ell!)^4}\Big(\frac{B}{2m_s\Omega_{cs}^2}\Big)^\ell\Big(\int\mathrm{d}\mathcal{W}F_{sM}\mu^\ell\Big)\nabla_\perp^{2\ell}\phi \\ &= n_{s0}\sum_{\ell=0}^\infty\frac{(2\ell)!}{(\ell!)^3}\Big(\frac{\rho_s^2}{2}\Big)^\ell\nabla_\perp^{2\ell}\phi = n_{s0}\Gamma_{0s}\phi,\end{aligned}$$

in which we recognized the series expansion of $\Gamma_{0s}(k_\perp^2\rho_s^2) = \sum_{\ell=0}^\infty[(2\ell)!/(\ell!)^3](\rho_s^2/2)^\ell\nabla_\perp^{2\ell}$.

at fixed ζ corresponds to advancing ϑ by one while decrementing ξ by q, so $f_s(V, \vartheta = 1/2, \xi - q/2) = f_s(V, \vartheta = -1/2, \xi + q/2)$. Due to periodicity in ξ, only the nonintegral portion of the shift (q) is significant. For a radially thin layer, we may linearize the radial variation of q but, since q is generally nonintegral, we must allow a nontrivial shift in ξ when one applies the poloidal periodicity constraint, even at the radial center of the domain.

Our parallel boundary conditions may be simplified in the fluxtube limit, for the following reason: To thin the number of modes retained on a given surface, we enforce periodicity in ξ at $1/n$ for some integer $n > 1$. When we do this, the poloidal periodicity becomes simple (unshifted) whenever nq is an integer. The fluxtube limit refers to the case $n \gg 1$, which allows us to assume (without further loss of generality) that we center our domain on a surface where nq is rational. In this case, we obtain the standard fluxtube parallel boundary conditions, with the shift in parallel boundary conditions following only from magnetic shear, linear (thus odd) in x about the center of the domain.

Our delta-f system of equations [Eqs. (15), (18), and (21)] nonlinearly conserve a free energy $(\sum_s U_{\delta s}) + U_{\delta E} + U_{\delta M}$, with thermal free energies $U_{\delta s} \doteq \int \mathrm{d}\Lambda\, T_{s0} f_s^2 / 2F_{sM}$, $\boldsymbol{E} \times \boldsymbol{B}$ free energy $U_{\delta E} \doteq \frac{1}{2} \int \mathrm{d}\mathcal{V} \sum_s n_{s0} Z^2 e^2 [\phi(1 - \Gamma_{0s})\phi]/T_{s0}$,[10] and magnetic energy $U_{\delta M} \doteq \int \mathrm{d}\mathcal{V}\, |\nabla_\perp A_\parallel|^2 / 8\pi$. Assuming boundary terms to vanish, which requires an appropriate choice of radial boundary conditions, the separate components evolve as[11,12]

$$\partial_t U_{\delta s} = \int \mathrm{d}\Lambda f_s \Big[-Zev_\parallel \Big(\frac{\partial_t J_0 A_\parallel}{c} + \nabla_\parallel J_0 \phi - \frac{\{J_0 A_\parallel, J_0 \phi\}}{B_0} \Big) + \frac{1}{2}(m_s v_\parallel^2 + \mu B) \mathcal{K}(J_0 \phi) + T_{s0} \frac{c}{B_0} \partial_y (J_0 \psi_e) \frac{F'_{sM}}{F_{sM}} \Big], \quad (22)$$

$$\partial_t U_{\delta E} = \sum_s \int \mathrm{d}\Lambda\, f_s \Big[Zev_\parallel \big(\nabla_\parallel J_0 \phi - B_0^{-1} \{J_0 A_\parallel, J_0 \phi\} \big) - 0.5 (m_s v_\parallel^2 + \mu B) \mathcal{K}(J_0 \phi) \Big], \quad (23)$$

$$\partial_t U_{\delta M} = c^{-1} \sum_s \int \mathrm{d}\Lambda\, Zev_\parallel f_s \partial_t J_0 A_\parallel . \quad (24)$$

Similarly to the full-F energy equations (9) and (10), the delta-f energies $U_{\delta s}$ and $U_{\delta E}$ may be seen to exchange energy based on the flow of plasma up or down ∇H_1, while $U_{\delta s}$ and $U_{\delta M}$ exchange energy due to flow with or against the inductive parallel electric field.

[10] Note that $1 - \Gamma_{0s}$ is a positive operator.

[11] Act on Eq. (18) with $\int \mathrm{d}\Lambda\, (T_{s0} f_s / F_{sM})$, on Eq. (21) with $\int \mathrm{d}\mathcal{V}\, \phi \partial_t$ [using Eq. (18) to substitute for $\partial_t f_s$], and on Eq. (15) with $-(4\pi)^{-1} \int \mathrm{d}\mathcal{V} (\partial_t A_\parallel)$. Use the facts that [for arbitrary spatial functions f_1 and f_2, and assuming compatible radial boundary conditions]: geometric factors depend only on s; F_{sM} and F'_{sM} depend only on s (via B), $v_\parallel$, and μ, and are even in $v_\parallel$; $\{\cdot,\cdot\}$ and $\mathcal{K}$ do not differentiate with respect to s; $\int \mathrm{d}x \int \mathrm{d}y \{f_1, f_2\} = \int \mathrm{d}x \int \mathrm{d}y\, \mathcal{K}(f_1) = 0$; $\int \mathrm{d}\mathcal{W} \nabla_\parallel = \int (\mathrm{d}\mathcal{W}/B) B_0 \partial_s$, where $\int \mathrm{d}\mathcal{W}/B$ is spatially constant, annihilates velocity-space derivatives, and commutes with spatial derivatives and integration; $\nabla_\perp^2$ is self-adjoint under $\int \mathrm{d}x \int \mathrm{d}y$, thus so are J_0 and Γ_{0s} (whose spatial coefficients depend only on s); J_0 and Γ_{0s} are independent of time and $v_\parallel$; $m_s v_\parallel \nabla_\parallel F_{sM} = (\mu \nabla_\parallel B) \partial_{v_\parallel} F_{sM}$.

[12] The $\mathcal{K}^x F'_{sM}$ term in the last row of Eq. (18) does not contribute to Eqs. (22) or (23) for the following reason: Only the x- and y-averaged portions of f_s or ϕ (respectively) can make a nonvanishing contribution. These evolve according to the x- and y-averaged Eqs. (18) and (21), written here with an overline to indicate the xy-average:

$$\partial_t \overline{f_s} + (Ze/c)(v_\parallel / T_{s0}) F_{sM} \partial_t \overline{A_\parallel} + v_\parallel \nabla_\parallel \overline{f_s} - m_s^{-1} (\mu \nabla_\parallel B) \partial_{v_\parallel} \overline{f_s} + (v_\parallel F_{sM} / T_{s0}) Ze \nabla_\parallel \overline{\phi} = (2Ze)^{-1} (\mu B + m_s v_\parallel^2) \mathcal{K}^x F'_{sM},$$

$$\sum_s \int \mathrm{d}\mathcal{W}\, Ze \overline{f_s} = 0.$$

This is a linear system, with no direct coupling to other modes. We therefore assume that finite-frequency modes have damped away, and solve for the steady-state solution. Considering first the odd-in-$v_\parallel$ portion of the steady-state equation (to which the even-in-$v_\parallel$ $\mathcal{K}^x F'_{sM}$ does not contribute), we find an even-in-$v_\parallel$ $\overline{f_s}$ with a nonvanishing gyrocenter density perturbation that is signed with $-Ze\overline{\phi}$, implying by the quasineutrality condition that $\overline{\phi}$ and the even-in-$v_\parallel$ $\overline{f_s}$ must vanish. The even-in-$v_\parallel$ portion of the equation contains the response to the (inhomogeneous) $\mathcal{K}^x F'_{sM}$ term, for which the steady-state $\overline{f_s}$ is odd in $v_\parallel$, automatically satisfying the Poisson equation. Since $\overline{\phi} = 0$ and $\overline{f_s}$ is odd in $v_\parallel$, the contributions of the $\mathcal{K}^x F'_{sM}$ term to Eqs. (22) and (23) vanish. [Collisional dissipation would allow a nonvanishing but small contribution of this term, proportional to the weak neoclassical heat flux, which we neglect relative to the turbulent one.]

2.3. Even/odd decomposition

In the delta-f free energy equations [Eqs. (22)–(24)], the dominant sources are even in $v_\parallel$, while many of the dissipation channels are odd in $v_\parallel$. For this reason, the flow of energy in phase space may be clarified with the decomposition $f_s = f_s^{\rm ev} + f_s^{\rm od}$, splitting apart the even $f_s^{\rm ev}(v_\parallel) \doteq [f_s(v_\parallel) + f_s(-v_\parallel)]/2$ and odd $f_s^{\rm od}(v_\parallel) \doteq [f_s(v_\parallel) - f_s(-v_\parallel)]/2$ portions.[13] Taking the even and odd portions of Eq. (18) yields the evolution equations:

$$\partial_t f_s^{\rm ev} + (c/B_0)\{J_0\phi, f_s^{\rm ev}\} - (m_s v_\parallel^2 + \mu B)\mathcal{K}(h_s^{\rm ev})/2Ze$$
$$+ v_\parallel \nabla_\parallel f_s^{\rm od} - B_0^{-1} v_\parallel \{J_0 A_\parallel, f_s^{\rm od}\} - m_s^{-1}(\mu \nabla_\parallel B)\partial_{v_\parallel} f_s^{\rm od}$$
$$= [(c/B_0)\partial_y(J_0\phi) + (\mu B + m_s v_\parallel^2)\mathcal{K}^x/2Ze]F'_{sM}, \quad (25)$$

$$\partial_t f_s^{\rm od} + (Zev_\parallel/cT_{s0})F_{sM}\partial_t J_0 A_\parallel + (c/B_0)\{J_0\phi, f_s^{\rm od}\}$$
$$+ v_\parallel \nabla_\parallel h_s^{\rm ev} - B_0^{-1} v_\parallel \{J_0 A_\parallel, h_s^{\rm ev}\} - m_s^{-1}(\mu\nabla_\parallel B)\partial_{v_\parallel} h_s^{\rm ev}$$
$$-(m_s v_\parallel^2 + \mu B)\mathcal{K}(f_s^{\rm od})/2Ze = -B_0^{-1} v_\parallel F'_{sM}\partial_y(J_0 A_\parallel), \quad (26)$$

in which $h_s^{\rm ev} \doteq f_s^{\rm ev} + (F_{sM}/T_{s0})ZeJ_0\phi$. The field equations are nearly unchanged:

$$\sum_s n_{s0} Z^2 e^2 \frac{1-\Gamma_{0s}}{T_{s0}}\phi = \sum_s \int \mathrm{d}\mathcal{W}\, ZeJ_0 f_s^{\rm ev}, \quad (27)$$

$$\nabla_\perp^2 A_\parallel = -\frac{4\pi}{c}\sum_s \int \mathrm{d}\mathcal{W}\, Zev_\parallel J_0 f_s^{\rm od}. \quad (28)$$

Using Eqs. (25)–(28), we can again derive free energy conservation laws, decomposing $U_{\delta s} = U_{\delta s}^{\rm ev} + U_{\delta s}^{\rm od}$ for $U_{\delta s}^{\rm ev} \doteq \int \mathrm{d}\Lambda\, T_{s0}(f_s^{\rm ev})^2/2F_{sM}$ and $U_{\delta s}^{\rm od} \doteq \int \mathrm{d}\Lambda\, T_{s0}(f_s^{\rm od})^2/2F_{sM}$:

$$\partial_t U_{\delta s}^{\rm ev} = \int \mathrm{d}\Lambda \Bigg[f_s^{\rm ev}\frac{1}{2}(m_s v_\parallel^2 + \mu B)\mathcal{K}(J_0\phi)$$
$$+ \frac{T_{s0}}{F_{sM}} f_s^{\rm od}\left[v_\parallel\left(\nabla_\parallel f_s^{\rm ev} - \frac{1}{B_0}\{J_0 A_\parallel, f_s^{\rm ev}\}\right) - \frac{\mu\nabla_\parallel B}{m_s}\partial_{v_\parallel} f_s^{\rm ev}\right]$$
$$+ f_s^{\rm ev} T_{s0}\frac{c}{B_0}\partial_y(J_0\phi)\frac{F'_{sM}}{F_{sM}}\Bigg], \quad (29)$$

$$\partial_t U_{\delta s}^{\rm od} = \int \mathrm{d}\Lambda \Bigg[-Zev_\parallel f_s^{\rm od}\left[\frac{\partial_t J_0 A_\parallel}{c} + \nabla_\parallel(J_0\phi) - \frac{\{J_0 A_\parallel, J_0\phi\}}{B_0}\right]$$
$$- \frac{T_{s0}}{F_{sM}} f_s^{\rm od}\left[v_\parallel\left(\nabla_\parallel f_s^{\rm ev} - \frac{1}{B_0}\{J_0 A_\parallel, f_s^{\rm ev}\}\right) - \frac{\mu\nabla_\parallel B}{m_s}\partial_{v_\parallel} f_s^{\rm ev}\right]$$
$$- f_s^{\rm od} v_\parallel T_{s0}\frac{1}{B_0}\partial_y(J_0 A_\parallel)\frac{F'_{sM}}{F_{sM}}\Bigg], \quad (30)$$

$$\partial_t U_{\delta E} = \sum_s \int \mathrm{d}\Lambda \left[-\frac{1}{2}(m_s v_\parallel^2 + \mu B) f_s^{\rm ev}\mathcal{K}(J_0\phi)\right.$$
$$\left. + Zev_\parallel f_s^{\rm od}[\nabla_\parallel(J_0\phi) - B_0^{-1}\{J_0 A_\parallel, J_0\phi\}]\right], \quad (31)$$

$$\partial_t U_{\delta M} = \frac{1}{c}\sum_s \int \mathrm{d}\Lambda\, Zev_\parallel f_s^{\rm od}\partial_t J_0 A_\parallel. \quad (32)$$

The free energy sources and transfer pathways of Eqs. (29)–(32) are sketched in Fig. 2. Although Eqs. (29) and (30) sum to Eq. (22), the split $U_{\delta s} \to U_{\delta s}^{\rm ev} + U_{\delta s}^{\rm od}$ will help elucidate the free energy transfer that drives a symmetry-breaking momentum flux.

[13] Here and throughout the section, we will often suppress the dependencies other than $v_\parallel$, since they are left unchanged when we take the even and odd (in $v_\parallel$) portions of f_s.

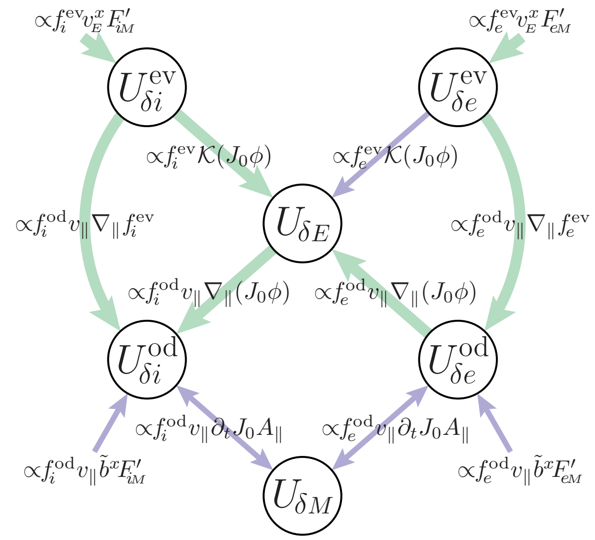

Figure 2. Free-energy flow in Eqs. (29)–(32), arrow heads indicating typical direction of energy transfer. Thick green arrows indicate the terms that dominate the energy flows in the low-frequency, low-$k_\perp$ scenario of Sec. 4.2. The transfer terms $\propto f_s^{\rm od} v_\parallel \nabla_\parallel f_s^{\rm ev}$ refer to the entire second rows of Eqs. (29) and (30). Contravariant component notation is used for $v_E^x \doteq \boldsymbol{v}_E \cdot \nabla x$ and the fluctuating magnetic direction $\tilde{b}^x = B_0^{-1}\partial_y(J_0 A_\parallel)$. The parallel gradient terms here also intend the nonlinear parallel gradients.

3. Symmetry

If one assumes an up-down symmetric magnetic geometry, no background toroidal rotation or rotation shear, and no background $\boldsymbol{E} \times \boldsymbol{B}$ shear, then the lowest-order fluxtube delta-f equations satisfy a symmetry that annihilates the statistically averaged leading-order radial flux of toroidal angular momentum [16]. In specific, if the functions $f_s(x, y, s, v_\parallel, \mu, t)$, $\phi(x, y, s, t)$, and $A_\parallel(x, y, s, t)$ jointly solve the nonlinear gyrokinetic system, then so do the functions $-f_s(-x, +y, -s, -v_\parallel, +\mu, +t)$, $-\phi(-x, +y, -s, +t)$, and $A_\parallel(-x, +y, -s, +t)$. However, the leading-order radial flux of toroidal angular momentum changes sign under this transform. Since the two solutions should occur with equal probability, one concludes that the radial flux of toroidal angular momentum must vanish in the statistical average. In this section, we will verify that our Eqs. (18), (21), and (15) satisfy the above symmetry, show that our leading-order momentum flux is odd under the transform, briefly discuss the role of neoclassical flows in symmetry breaking, and identify a "skew-ness" in the symmetry transform that will lead to our residual stress in Sec. 4.

For an up-down symmetric magnetic geometry, our geometric coefficients are straightforwardly found[14] to satisfy $B(-s) = B(s)$, $\mathcal{K}^x(-s) = -\mathcal{K}^x(s)$, $\mathcal{K}^y(-s) = \mathcal{K}^y(s)$, $g^{xx}(-s) = g^{xx}(s)$, $g^{xy}(-s) = -g^{xy}(s)$, and $g^{yy}(-s) = g^{yy}(s)$. Since $\nabla_\perp^2$ vanishes for all equilibrium quantities (which depend only on s in the radially local geometry), it is easily verified that $\nabla_\perp^2$ is invariant under the transformation, which inverts the sign of ∂_x but not of ∂_y. The equilibrium distribution F_{sM} and its gradient F'_{sM} are also both invariant under the transform, since both are independent of x and are even in $v_\parallel$ and s. Invariance of $\nabla_\perp^2$, F_{sM}, and B under the transform jointly imply that the Bessel operators J_0 and Γ_{0s} are also invariant. Substitution of the transformed functions into Eqs. (18), (21), and (15) then reproduces the original equations,[15] which implies (assuming compatible boundary conditions) that for every solution $[f_s(x, y, s, v_\parallel, \mu, t),\ \phi(x, y, s, t),\ A_\parallel(x, y, s, t)]$, the corresponding transformed functions $[-f_s(-x, +y, -s, -v_\parallel, +\mu, +t),\ \ -\phi(-x, +y, -s, +t),\ A_\parallel(-x, +y, -s, +t)]$ also constitute a solution.

Compatibility of boundary conditions is not a trivial requirement, and is generally satisfied only if one makes the (fluxtube) approximation of toroidal periodicity at $\xi = 1/n$ for integer $n \gg 1$: Recall that the true (full flux-surface) poloidal (s) boundary conditions are shifted-periodic $f_s(x, \vartheta = 1/2, \xi - q(x)/2) = f_s(x, \vartheta = -1/2, \xi + q(x)/2)$, where only the nonintegral part of q is significant (due to perodicity in ξ). If we truncate our toroidal domain at $\xi = 1/n$ for integer $n > 1$, these boundary conditions remain formally unchanged, but now only the nonintegral part of (nq) is significant. If we apply the symmetry transform ($x \to -x$, $\vartheta \to -\vartheta$, $\xi \to +\xi$) to some function, the transformed function would satisfy the boundary conditions $f_s(-x, \vartheta = -1/2, \xi - q(x)/2) = f_s(-x, \vartheta = 1/2, \xi + q(x)/2)$, equivalently written as $f_s(x, \vartheta = 1/2, \xi + q(-x)/2) = f_s(x, \vartheta = -1/2, \xi - q(-x)/2)$. These transformed boundary conditions are equivalent to the actual ones only if the shift $q(x)$ is odd in x, an assumption that we can only make if we take the $n \gg 1$ limit, as we discussed towards the end of Sec. 2.2. For this reason, only the fluxtube limit (not simply radial locality) is enough to imply the validity of this symmetry argument.

Assuming compatible boundary conditions, it remains to be shown that our leading-order momentum flux changes sign under the symmetry transform. Decomposing $F_s \to f_s + F_{sM}$ in Eq. (12) and using the leading-order fluxtube approximations to the characteristics $(\dot{\boldsymbol{R}} \cdot \nabla x) \to [-(c/B_0)\partial_y(J_0\psi_e) - (m_s v_\parallel^2 + \mu B)\mathcal{K}^x/2Ze]$ [c.f. Eq. (16) and following], we obtain the leading-order flux-surface-averaged contravariant x-component of the flux of parallel toroidal angular momentum as $-\langle f_s m_s v_\parallel b_\varphi[(c/B_0)\partial_y(J_0\psi_e) + (m_s v_\parallel^2 + \mu B)\mathcal{K}^x/2Ze]\rangle - \langle F_{sM} Ze(J_0 A_\parallel) b_\varphi B_0^{-1} \partial_y(J_0\phi)\rangle$.[16] Evaluating this momentum flux with the transformed solution changes its sign, implying that it should vanish in the average for solutions determined with our delta-f system of equations.[17] Interestingly, the (local) divergence of this radial momentum flux is invariant under the transform, since $\partial_x \to -\partial_x$. The invariance of this (physically insignificant) local divergence does not contradict the general argument, since the averaged radial flux divergence is zero, due to the statistical radial homogeneity that follows from radial locality.[18] In fact, one may conclude that the radial momentum transport due to the leading-order Reynolds and Maxwell stress must vanish in the average because its divergence $[\langle Zef_s\partial_\varphi(J_0\psi_e)\rangle]$ is invariant under the transform,[19] which takes $x \to -x$, so the undifferentiated radial fluxes must flip sign.[20]

[14] The Hamada angle ζ is equal to $\varphi/2\pi$ plus an axisymmetric function. For an up-down symmetric magnetic geometry, this axisymmetric function may be chosen odd in θ.

[15] As one approach, evaluate the equations for the transformed functions at the point $(-x, +y, -s, -v_\parallel, +\mu, +t)$, then express everything in terms of the original functions and the geometric coefficients all evaluated at the point $(x, y, s, v_\parallel, \mu, t)$.

[16] Note that the nonlinear contribution of the fluctuating electromagnetic parallel toroidal angular momentum is subdominant to the mechanical one, by

$$\frac{f_s(Ze/c)J_0A_\parallel}{f_s m_s v_\parallel} \sim \frac{ZeA_\parallel}{cm_s v_{ts}}\frac{k_\perp B}{k_\perp B} \sim \frac{1}{k_\perp \rho_s}\frac{k_\perp A_\parallel}{B} \ll 1.$$

The $F_{sM}A_\parallel$ term that we retain is formally of the same order as the mechanical parallel momentum term, but note that only FLR-correction portions of the $F_{sM}A_\parallel$ term survive, due to leading-order charge neutrality.

[17] If we consider a "local flux-surface average" [taking $\langle\cdots\rangle \to (V')^{-1}\oint \mathrm{d}s \oint \mathrm{d}y$ in the local variables] then, strictly speaking, this argument only shows that the statistical average of the flux-surface-averaged momentum flux terms must be odd in x, thus that its x integral must vanish. [Specific boundary conditions in x may allow stronger conclusions. For example, periodic boundary conditions in x should make the system translation-invariant in x, allowing us to conclude that the momentum flux terms vanish separately at each flux surface (in the statistical average).] However, recalling that our delta-f model is radially local, it is actually the full domain integral of the delta-f result that corresponds to the flux-surface average in the global model.

[18] Statistical radial homogeneity within the flux tube only strictly holds if suitable boundary conditions in x are chosen (e.g. periodic). However, radial variation within the flux tube (including a nonvanishing momentum flux divergence within the local domain) is not physically meaningful, resulting purely from the (artificial) local radial boundary conditions. The divergence of the radial momentum flux in Eq. (12) should be interpreted using the difference between the domain-integrated local momentum flux in two radially nearby local domains.

[19] Simple toroidal derivatives ∂_φ are proportional to ∂_y, thus are invariant under the transform.

[20] The logic in the main text is not quite complete, since a momentum flux divergence that is statistically even in x may arise from a momentum flux that includes a (nonzero) term that is statistically constant in x. However, this

As an interesting aside: Eq. (18) retains the curvature drift acting on the background Maxwellian, thus includes the first-order neoclassical flows. These are solved for together with the turbulent fluctuations, so the resulting turbulent flux includes corresponding effects of the neoclassical disturbance to the background Maxwellian. Despite this fact, the leading-order momentum flux is constrained by the symmetry argument to vanish. This suggests that the neoclassical flows alone are not able to give rise to nonvanishing turbulent residual stress, in an otherwise leading-order delta-f system. Although Eq. (18) does not explicitly include collisions, any sensible linear collision operator will be invariant under the symmetry transform, leaving this result intact. The introduction of an inhomogeneous (but radially constant) neoclassical radial electrical field will also not disturb the result, since it would be invariant to the transform, just like the radial electric field we have retained, $-\partial_x\phi$. However, profile curvature, background radial electric field shear, and higher-order terms like nonlinear parallel acceleration would violate the leading-order symmetry and are therefore not prohibited from causing residual stress, although a self-consistent radially global treatment may expose constraints on their contributions.

Before moving on, we highlight a necessary skewness of the coordinate transformation, which will lead to the symmetry breaking discussed in the next section. As sketched in Fig. 3(a), the covariant poloidal direction $\partial_\vartheta|_{V,\xi}\boldsymbol{R} \propto \partial_s\boldsymbol{R}$ is aligned with the (equilibrium) magnetic field, which must happen since both ∇x and ∇y are orthogonal to $\hat{\boldsymbol{b}}$. This is the

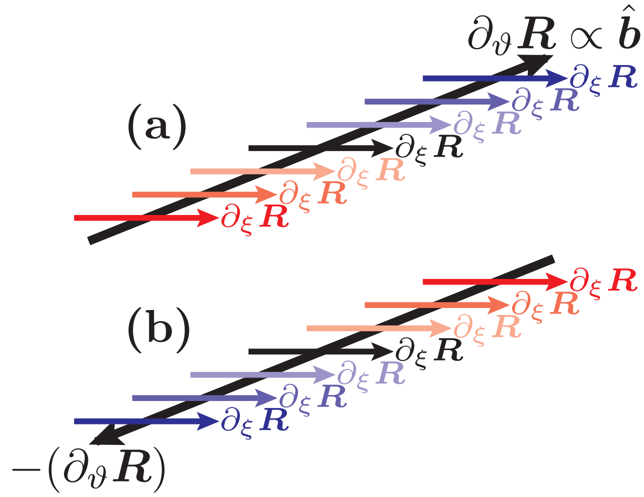

Figure 3. (a) Sketch of the covariant poloidal ($\partial_\vartheta\boldsymbol{R}$) and binormal ($\partial_\xi\boldsymbol{R}$) directions. The horizontal direction is toroidal. Alignment of $\partial_\xi\boldsymbol{R}$ with the toroidal direction is the reason that $\partial_\xi|_{V,\vartheta} = (\partial_\xi\boldsymbol{R})\cdot\nabla$ captures only toroidal variation. (b) Sketch of the effective transformations of the covariant vectors, showing that while the parallel gradient $\hat{\boldsymbol{b}}\cdot\nabla \propto (\partial_\vartheta\boldsymbol{R})\cdot\nabla = \partial_\vartheta|_{V,\xi}$ clearly changes sign under the transform, the perpendicular gradient within the flux surface is composed of a linear combination of $(\partial_\vartheta\boldsymbol{R})\cdot\nabla$ (which changes sign) and $(\partial_\xi\boldsymbol{R})\cdot\nabla$ (which has unchanged sign). This implies that $\boldsymbol{E}_\perp$ has no definite parity under the transform, which causes the symmetry breaking that we derive in Sec. 4.

reason that $\partial_\vartheta = (\partial_\vartheta\boldsymbol{R})\cdot\nabla$ is proportional to $\nabla_\parallel$, thus captures only slow spatial variation, allowing us to order $\partial_s \ll k_\perp$. The covariant binormal direction $\partial_\xi|_{V,\vartheta}\boldsymbol{R} \propto \partial_y\boldsymbol{R}$ is aligned with the toroidal direction. This choice means that $\partial_\xi = (\partial_\xi\boldsymbol{R})\cdot\nabla$ captures only toroidal variation and vanishes for axisymmetric quantities. Simple periodicity in y also follows directly from the purely toroidal orientation of $\partial_\xi\boldsymbol{R}$, combined with physical toroidal periodicity. All of these properties were necessary for the construction of the radially local delta-f system and the resulting symmetry argument. However, they imply that while the parallel gradient simply changes sign under the symmetry transform, the perpendicular gradient (and therefore the perpendicular electric field) does not have a definite parity [Fig. 3(b)], a result that follows directly from the fact that $\hat{\boldsymbol{b}}$ is not orthogonal to $\nabla\varphi$. This skewness causes the symmetry breaking that we will now derive.

4. Symmetry Breaking

In this section, we will discuss the geometry of the radial $\boldsymbol{E}\times\boldsymbol{B}$ drift and the resulting symmetry breaking in a simple, pictorial way. We will identify a portion of the $\boldsymbol{E}\times\boldsymbol{B}$ drift, small in the delta-f orderings, that contributes a momentum flux that is invariant to the symmetry transformation presented

possibility may be ruled out by examining a procedure to actually derive the undifferentiated momentum flux. By adding $0 = \langle Zef_s\partial_\varphi(\psi_e - \psi_e)\rangle + \langle Ze(J_0 f_s - J_0 f_s)\partial_\varphi\psi_e\rangle$, rearranging, integrating by parts as needed in φ, and using Eqs. (21) and (15), we obtain

$$-\langle Zef_s\partial_\varphi(J_0\psi_e)\rangle = \langle Zef_s\partial_\varphi(1-J_0)\psi_e\rangle + \langle\psi_e\partial_\varphi(1-J_0)Zef_s\rangle + \sum_s (n_{s0}/T_{s0})Z^2e^2\,\langle\phi\partial_\varphi(1-\Gamma_{0s})\phi\rangle + (4\pi)^{-1}\langle A_\parallel\partial_\varphi\nabla_\perp^2 A_\parallel\rangle$$

Each of the Bessel operators $(1-J_0)$ and $(1-\Gamma_{0s})$ may be cast as an ascending power series in $\nabla_\perp^2$, beginning with $(\nabla_\perp^2)^1$. Neglecting perpendicular variation of the (axisymmetric) coefficients of these expansions (by the radially local orderings), the problem is thus reduced to manipulation of terms of the analogous forms $[f_s\partial_\varphi\nabla_\perp^{2\ell}\psi_e + \psi_e\partial_\varphi\nabla_\perp^{2\ell}f_s]$, $[\phi\partial_\varphi\nabla_\perp^{2\ell}\phi]$, and $[A_\parallel\partial_\varphi\nabla_\perp^2 A_\parallel]$, for $\ell \geq 1$. Repeated integrations by parts on the Laplacians allow us to recast each of these terms as a linear combination of total divergences and total toroidal partials, the latter of which vanish under the flux surface average. The total divergences may be recast using the radially local flux-surface property $\langle\nabla\cdot\boldsymbol{w}\rangle = \partial_x\langle\boldsymbol{w}\cdot\nabla x\rangle$ (for arbitrary vector $\boldsymbol{w}$). The general form of the undifferentiated flux terms (the various instances of $\boldsymbol{w}\cdot\nabla x$) shows that all of them flip sign under the transformation, allowing one to unambiguously conclude that the leading-order undifferentiated momentum flux corresponding to $\langle Zef_s\partial_\varphi(J_0\psi_e)\rangle$ is statistically odd in x, thus vanishes under the domain integral.

in Sec. 3. The symmetry argument therefore does not prevent the solution of our delta-f model from driving a residual stress via this term. Further, we will find that the resulting momentum flux term is proportional to a free-energy transfer term that appears in the leading-order delta-f formulation of Secs. 2.2 and 2.3. That free-energy term plays a definite role in the free-energy balance for low-$k_\perp$, low-frequency turbulence, which causes it to have a preferred sign and a nonzero average, even in fully nonlinear, saturated turbulence. Due to the correspondence of forms between the momentum flux and free-energy transfer terms, this symmetry breaking causes a definitely-signed momentum flux in real space, in particular transferring co-current momentum in the radially outward direction, leading to counter-current toroidal rotation peaking in the core.

4.1. Geometry of the $\boldsymbol{E}\times\boldsymbol{B}$ Drift

The symmetry breaking results from a skewness in the symmetry transform, as we discussed in the previous section. We will concretely evaluate this symmetry breaking and the resulting momentum flux using a simple, geometric formulation. Although we will write things in terms of our local flux-tube coordinates x, y, and s, our analysis rests on only the few properties that we list now, all of which are necessary for the construction of the delta-f geometry and its symmetry properties: Since the geometry is axisymmetric with good nested flux surfaces, we may specify radial position with a flux-surface label x, which is axisymmetric and satisfies $\hat{\boldsymbol{b}}\cdot\nabla x = 0$. Poloidal position is specified by a distended but axisymmetric poloidal angle label s. The binormal coordinate y is chosen so that $\hat{\boldsymbol{b}}\cdot\nabla y = 0$, allowing it to label perpendicular position within the flux surface. These choices are necessary for our symmetry arguments: The definition of y allows us to conclude that $\hat{\boldsymbol{b}}\cdot\nabla = (\hat{\boldsymbol{b}}\cdot\nabla s)\partial_s$ so $\partial_s|_{x,y} = (\hat{\boldsymbol{b}}\cdot\nabla s)^{-1}\hat{\boldsymbol{b}}\cdot\nabla$ captures only slow variation, a fact that is used in the delta-f orderings. The choice of an axisymmetric poloidal coordinate s, combined with the necessarily axisymmetric definition of x, implies that the partial $\partial_y|_{x,s}$ is proportional to a simple toroidal derivative ($\hat{\boldsymbol{\varphi}}\cdot\nabla$ for $\hat{\boldsymbol{\varphi}} \doteq R\nabla\varphi$), since holding x and s fixed is equivalent to holding R and vertical position z fixed. This property implies that that $\partial_y|_{x,s}$ vanishes (exactly) for any axisymmetric quantity and that toroidal periodicity implies simple periodicity in y, both facts that we used in deriving the structure of the radially local geometry (Sec. 2.2) and the symmetry transform's constraints on momentum flux (Sec. 3).

Consider next the contribution of the neglected portion of the $\boldsymbol{E}\times\boldsymbol{B}$ drift in a simple, geometric way. Defining the radial and poloidal directions $\hat{\boldsymbol{x}} \doteq (\nabla x)/|\nabla x|$ and $\hat{\boldsymbol{p}} \doteq \hat{\boldsymbol{\varphi}}\times\hat{\boldsymbol{x}}$, decompose $\hat{\boldsymbol{b}} = b_T\hat{\boldsymbol{\varphi}} + b_p\hat{\boldsymbol{p}}$. Since $\hat{\boldsymbol{x}}\times\hat{\boldsymbol{b}} = (\hat{\boldsymbol{\varphi}} - b_T\hat{\boldsymbol{b}})/b_p$, the radial component of the $\boldsymbol{E}\times\boldsymbol{B}$ drift is

$$\boldsymbol{v}_E\cdot\hat{\boldsymbol{x}} = \frac{c}{B}\hat{\boldsymbol{b}}\times\nabla(J_0\phi)\cdot\hat{\boldsymbol{x}} = \frac{c}{b_pB}(\hat{\boldsymbol{\varphi}} - b_T\hat{\boldsymbol{b}})\cdot\nabla(J_0\phi), \tag{33}$$

c.f. the upper left of Fig. 4. For the momentum flux [Eq. (12)], we actually need the contravariant radial component of the $\boldsymbol{E}\times\boldsymbol{B}$ drift, which we may write as[21]

$$v^x_E \doteq \boldsymbol{v}_E\cdot\nabla x = v^x_{E1} + v^x_{E2}, \tag{34}$$

for

$$v^x_{E1} \doteq -\frac{c}{B_0}\partial_y(J_0\phi), \qquad v^x_{E2} \doteq \frac{c}{B}b_y\partial_s(J_0\phi), \tag{35}$$

in which $b_y \doteq \hat{\boldsymbol{b}}\cdot\partial_y|_{x,s}\boldsymbol{R} = -2\pi R b_T L_\parallel/V' \sim -b_T/b_p$ is the covariant y component of the magnetic direction. In either Eq. (33) or (34), the first term is the leading-order contribution. The symmetry arguments in Sec. 3 demonstrated that the statistically averaged radial flux of parallel toroidal angular momentum due to this term must vanish, when calculated with the solution of the delta-f equations given in Sec. 2.2. The second term [v^x_{E2} in Eq. (34)] is smaller than the first term by $k_\parallel/(k_\perp b_p)$, thus is neglected in Eq. (18). This term represents neither true parallel physics nor particle acceleration, rather it simply cancels the parallel gradient contribution that was incorrectly included in the first term, leaving the true $\nabla_\perp(J_0\phi)$, as is needed for a geometrically exact evaluation of the radial $\boldsymbol{E}\times\boldsymbol{B}$ drift. The domain-averaged contribution of v^x_{E2} to the radial flux of mechanical parallel toroidal angular momentum is given by $\Pi^{(2)}_\varphi = \sum_s \Pi^{(2)}_{\varphi s}$ for[22]

$$\begin{aligned}\Pi^{(2)}_{\varphi s} &\doteq V_{\rm pl}^{-1}\int \mathrm{d}\Lambda\, f_s m_s v_\parallel b_\varphi v^x_{E2} \\ &= \frac{1}{V_{\rm pl}}\frac{-2\pi c}{B^\theta V'}\int \mathrm{d}\Lambda\, f_s m_s v_\parallel b_\varphi^2 \nabla_\parallel J_0\phi,\end{aligned} \tag{36}$$

with $V_{\rm pl}$ the domain volume. Noting that $b_\varphi(+s) = b_\varphi(-s)$ for an up-down symmetric magnetic geometry, it is readily verified that $\Pi^{(2)}_{\varphi s}$ is invariant under the symmetry transform, thus is not restricted from driving a residual stress. Further, as we will now show, the connection of this term with the free energy flux will actually force it to break symmetry and drive residual stress in parameter regimes where there is significant energy transfer to ion parallel flows.

[21] From Sec. 2.2, recall the Clebsch form $\boldsymbol{B} = B_0\nabla x\times\nabla y$ and the unit Jacobian $(\nabla x\times\nabla y\cdot\nabla s)^{-1} = 1$, which lead to

$$\begin{aligned}\boldsymbol{v}_E\cdot\nabla x &= (c/B^2)\boldsymbol{B}\cdot[(\partial_y J_0\phi)\nabla y + (\partial_s J_0\phi)\nabla s]\times\nabla x \\ &= -(c/B_0)\partial_y(J_0\phi) + (c/B)(\partial_s J_0\phi)\hat{\boldsymbol{b}}\cdot\partial_y\boldsymbol{R}.\end{aligned}$$

[22] Note that the global flux-surface averages used in the full-F Eq. (12) correspond to a full domain average in the radially local Eq. (36).

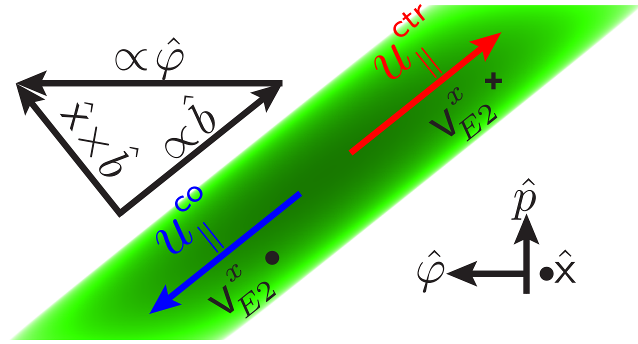

Figure 4. Side view of a toroidally asymmetric low-frequency fluctuation, with darker shading again showing larger $\tilde{n}_i$, proportional to $\tilde{\phi}$ by the low-$k_\perp$ electron adiabatic response. At frequencies $\lesssim k_\parallel v_{ti}$, ions flow along $\hat{\boldsymbol{b}}$ out of the density hump. The radial $\boldsymbol{E}\times\boldsymbol{B}$ drift, proportional to $\hat{\boldsymbol{x}}\times\hat{\boldsymbol{b}}\cdot\nabla(J_0\phi)$ is decomposed into a part v_{E1}^x due to toroidal potential variation $(\hat{\boldsymbol{\varphi}}\cdot\nabla\phi)$ and a part v_{E2}^x due to parallel potential variation $(\hat{\boldsymbol{b}}\cdot\nabla\phi)$. Although v_{E1}^x (not shown) is now nonzero, its leading-order contribution to the momentum flux vanishes by symmetry. The correction term v_{E2}^x breaks the symmetry and brings counter-(co-)current parallel momentum inwards (outwards).

4.2. Free energy and momentum fluxes

As we have stressed, the symmetry-breaking momentum flux $\Pi_\varphi^{(2)}$ results simply from the $\boldsymbol{E}\times\boldsymbol{B}$ advection of parallel toroidal angular momentum, with $\nabla_\parallel(J_0\phi)$ appearing due to a symmetry-breaking correction v_{E2}^x to the leading-order fluxtube approximation for the $\boldsymbol{E}\times\boldsymbol{B}$ drift. Nevertheless, $\Pi_{\varphi s}^{(2)}$ has a very similar form to the domain-averaged term

$$T_{\phi s}^{\parallel} \doteq -\int\frac{\mathrm{d}\Lambda}{V_{\mathrm{pl}}} Zev_\parallel f_s \nabla_\parallel J_0\phi = -\int\frac{\mathrm{d}\Lambda}{V_{\mathrm{pl}}} Zev_\parallel f_s^{\mathrm{od}} \nabla_\parallel J_0\phi, \quad (37)$$

which appears in Eqs. (22) and (30) and captures free energy transfer from the potential ($U_{\delta E}$) to parallel flows ($U_{\delta s}^{\mathrm{od}}$) via electrostatic parallel acceleration. [This energy transfer is sometimes referred to as "Landau damping" in kinetic wave calculations. This must be distinguished from "Landau closure," which refers to dissipative terms added to gyrofluid models to model the kinetic damping of higher moments by phase mixing.] The integrand in $T_{\phi s}^{\parallel}$ is almost directly proportional to that of $\Pi_{\varphi s}^{(2)}$, which differs only by a species-dependent constant factor times the $b_\varphi^2 = b_T^2 R^2 \approx R^2$ weighting, approaching a constant factor for large aspect ratio. Noting that $\Pi_\varphi^{(2)}$ is dominated by the ion contribution $\Pi_{\varphi i}^{(2)}$, and assuming either large aspect ratio or a not-too-strong poloidal variation of the energy transfer terms, a net free energy transfer from the potential $U_{\delta E}$ into ion parallel flows $U_{\delta i}^{\mathrm{od}}$, equivalent to $T_{\phi i}^{\parallel} > 0$, implies that $\Pi_\varphi^{(2)}$ will be nonzero with the sign of B^θ, equivalent to the sign of the toroidal plasma current I_p, corresponding to a radially outward flux of co-current momentum.

Why should we expect net energy transfer to ion parallel flows? The answer follows quite simply from the structure of the energy equations for the decomposition of f_s into its even-in-$v_\parallel$ ("state") portion f_s^{ev} and odd-in-$v_\parallel$ ("flux") portion f_s^{od}, as derived in Sec. 2.3. The background Maxwellian F_{sM} and its radial gradient F'_{sM} are even in $v_\parallel$. For this reason, the even portion of the free energy ($U_{\delta s}^{\mathrm{ev}}$) contains by far the dominant energy source, resulting from the $\boldsymbol{E}\times\boldsymbol{B}$ heat flux down the profile gradients $\int \mathrm{d}\Lambda\, f_s^{\mathrm{ev}} T_{s0}(c/B_0)\partial_y(J_0\phi)(F'_{sM}/F_{sM})$. In contrast, the odd portion of the free energy ($U_{\delta s}^{\mathrm{od}}$) has only the typically weak source due to magnetic flutter transport $-\int \mathrm{d}\Lambda f_s^{\mathrm{od}} v_\parallel T_{s0} B_0^{-1}\partial_y(J_0 A_\parallel)(F'_{sM}/F_{sM})$. Since much of the free energy dissipation acts on $\sum_s U_{\delta s}^{\mathrm{od}}$ while the dominant source is in $\sum_s U_{\delta s}^{\mathrm{ev}}$, a steady-state energy balance will require nonvanishing free energy transfer from $\sum_s U_{\delta s}^{\mathrm{ev}}$ to $\sum_s U_{\delta s}^{\mathrm{od}}$. Consulting Eqs. (29)–(31) and Fig. 2, there are only two basic transfer channels to accomplish this. First, there is a direct transfer mechanism, related to parallel flow generation by the parallel pressure gradient, that is given in the equal-and-opposite second rows of Eqs. (29) and (30). These terms have no counterpart in the fluxes on the RHS of Eq. (12), thus do not result in a symmetry-breaking momentum flux. However, there is also an indirect transfer mechanism, passing energy from $U_{\delta s}^{\mathrm{ev}}$ through $U_{\delta E}$, then completing the energy transfer to parallel flows by electrostatic parallel acceleration $T_{\phi s}^{\parallel}$, which due to the close relation to $\Pi_{\varphi s}^{(2)}$ is indeed capable of causing momentum flux.

Let's consider a typical scenario for this second energy-transfer pathway: Recall first that due to the electrons' small mass, their contribution to $\Pi_\varphi^{(2)}$ (and to the toroidal momentum flux in general) is quite small.[23] So, in order for $\Pi_\varphi^{(2)}$ to take significant values, the free energy transfer terms must act to excite ion parallel flows ($T_{\phi i}^{\parallel} \neq 0$). It is very difficult for this to occur unless there are potential fluctuations at frequency scales $\omega \lesssim k_\parallel v_{ti} \sim v_{ti}/qR$, since at higher frequencies there are very few ions in resonance with the parallel phase velocity $\omega/k_\parallel$. We may estimate turbulent frequencies roughly with the drift frequency $\omega \sim k_\perp \rho_i v_{ti}/L_\perp$, for $L_\perp$ the plasma gradient scale length, of order the device minor radius a for typical core turbulence. In that case, we see that our low-frequency requirement will typically be satisfied only for low $k_\perp$ fluctuations, $k_\perp\rho_i \lesssim L_\perp/qR$, about $k_\perp\rho_i \lesssim$

[23] Note also that unlike $T_{\phi s}^{\parallel}$, there is no factor of species charge Z in $\Pi_{\varphi s}^{(2)}$, so we expect ion and electron contributions to add in $\sum_s \Pi_{\varphi s}^{(2)}$ for the common case that they approximately cancel in $\sum_s T_{\phi s}^{\parallel}$. However, the electron contribution is smaller by at least $\sim (m_e/m_i)^{1/2}$, so we neglect it.

$|b_p|$ in the core. For the typical tokamak case $b_p = B_p/B \ll 1$, these $k_\perp$ are low enough that $J_0 \approx 1$ and $\Gamma_{0s} \approx 1$. Further, these frequencies are so low compared to electron parallel transit that electrons approximate adiabatic response, $\tilde{f}_e^{\rm ev} \approx F_{eM} e\tilde{\phi}/T_{e0}$. In this case, energy transfer from $U_{\delta e}^{\rm ev}$ into $U_{\delta e}^{\rm od}$ via the second row of Eq. (30) for electrons is approximately cancelled by transfer from $U_{\delta e}^{\rm od}$ to $U_{\delta E}$ via $T_{\phi e}^{\parallel} < 0$ [in the first row of Eq. (30)].[24] The energy is then transferred from $U_{\delta E}$ to ion parallel flows $U_{\delta i}^{\rm od}$ via $T_{\phi i}^{\parallel} > 0$. This final transfer will result in a radially outward flux of co-current momentum via $\Pi_\varphi^{(2)}$. The dominant energy pathways for this regime are sketched with thick green arrows in Fig. 2.

As an alternate viewpoint, note that for approximately adiabatic electrons and $k_\perp \rho_i \ll 1$, the Poisson equation constrains the ion gyrocenter density to be $\tilde{n}_i/n_{i0} \approx e\tilde{\phi}/T_{e0}$ (although it does not restrict the fluctuating ion temperature or detailed shape of the ion distribution function). In this case, density fluctuations may cause a correlation between ion pressure fluctuations and $\tilde{\phi}$, so that the ∼parallel ion pressure acceleration captured by the second row of Eq. (30) will typically be accompanied by an electrostatic ion parallel acceleration due to $T_{\phi i}^{\parallel}$ [in the first row of Eq. (30)], so that the net nonvanishing energy transfer into $U_{\delta i}^{\rm od}$ comes partially from $T_{\phi i}^{\parallel} > 0$, resulting in nonzero $\Pi_\varphi^{(2)}$ with the sign of I_p.[25]

The energy transfer term $T_{\phi i}^{\parallel}$ contains contributions from axisymmetric as well as nonaxisymmetric portions of f_i and ϕ. The axisymmetric portion captures an energy transfer involved in geodesic acoustic mode (GAM) damping, as sketched in Fig. 1 and discussed in detail in Ref. [23]. In the present notation, the GAM energy pathway appears as follows: Turbulent Reynolds stress excites a zonal $\boldsymbol{E} \times \boldsymbol{B}$ flow, the kinetic energy of which is contained in the axisymmetric part of $U_{\delta E}$. The $\boldsymbol{E} \times \boldsymbol{B}$ compressibility (due to ∇B) results in an energy transfer to density fluctuations, acting here via the $\mathcal{K}(J_0\phi)$ term in $\partial_t U_{\delta s}^{\rm ev}$.[26] Due to the low-$k_\perp$ adiabatic electron response, the resulting parallel density gradient is matched by a parallel electric field, which transfers energy to ion parallel flows, corresponding to $T_{\phi i}^{\parallel} > 0$ and causing a radial outflux of co-current momentum via $\Pi_\varphi^{(2)}$.

To close this section, we may use the above analysis to derive a scaling for the spin-up resulting from $\Pi_\varphi^{(2)}$. We assume that a fraction $0 \leq f_L \leq 1$ of the free energy is transferred to ion parallel flows by $T_{\phi i}^{\parallel}$.[27] Although f_L must generally be determined by numerical simulation, it will tend to be order-unity for low-frequency turbulence $\omega \lesssim k_\parallel v_{ti}$ and very small for higher-frequency turbulence $\omega \gg k_\parallel v_{ti}$. The domain-averaged free energy source may be estimated as $V_{\rm pl}^{-1} \sum_s \int {\rm d}\Lambda\, f_s \frac{c}{B_0} \partial_y (J_0 \psi_e) T_{s0} F'_{sM}/F_{sM} \sim \sum_s Q_s/L_{Ts}$, for Q_s and L_{Ts} respectively the species' heat flux and temperature gradient scale length. If a fraction f_L of this passes through $T_{\phi i}^{\parallel}$, then $T_{\phi i}^{\parallel} \sim f_L \sum_s Q_s/L_{Ts} \sim f_L Q/L_\perp$, so we get a domain-averaged residual stress around

$$\Pi_\varphi^{(2)} \sim \frac{2\pi m_i c}{ZeB^\theta V'} R^2 T_{\phi i}^{\parallel} \sim f_L \frac{R}{\Omega_{ci\theta}} \sum_s \frac{Q_s}{L_{Ts}} \sim f_L \frac{\rho_{i\theta}}{L_\perp} \frac{QR}{v_{ti}}, \quad (38)$$

for $\rho_{i\theta} \doteq v_{ti}/|\Omega_{ci\theta}|$, $v_{ti} \doteq (T_{i0}/m_i)^{1/2}$, and (signed) $\Omega_{ci\theta} \doteq ZeB_p/m_i c$. To estimate the magnitude of the core rotation peaking, we need to balance this residual stress against viscous saturation: Let U_φ be the core rotation peaking Mach number, with $U_\varphi v_{ti}$ roughly defined as toroidal rotation at the $q = 1$ surface minus toroidal rotation at the pedestal top. Taking $Q_i \to \chi_i n_{i0} T_{i0}/L_{Ti}$, $Q_e \to \chi_e n_{e0} T_{e0}/L_{Te}$, and viscous momentum flux to $\chi_\varphi n_{i0} m_i R U_\varphi v_{ti}/L_\varphi$ for transport coefficients χ_i, χ_e, and χ_φ, we may balance the angular momentum fluxes:

$$\chi_\varphi \frac{n_{i0} m_i R U_\varphi v_{ti}}{L_\varphi} = -\Pi_\varphi^{(2)} \sim -f_L \frac{R}{\Omega_{ci\theta}} \sum_s \chi_s \frac{n_{s0} T_{s0}}{L_{Ts}^2}. \quad (39)$$

If we then assume $\chi_\varphi \sim \chi_i$ and (for simplicity) $\chi_i \sim \chi_e$, $L_{Ti} \sim L_{Te} \sim L_\varphi \to L_\perp$, $n_{i0} \sim n_{e0}$, $T_{e0} \sim T_{i0}$, we get the simple estimate

$$U_\varphi \sim -f_L \frac{v_{ti}}{\Omega_{ci\theta} L_\perp}, \quad (40)$$

or, using Ampere's Law $2\pi r B_p \sim 4\pi I_p/c$ and assuming $Z=1$,

$$U_\varphi v_{ti} \sim -5 f_L \frac{T_0(\text{keV})}{I_p\,(\text{MA})} \frac{r}{L_\perp} \text{km/s}, \quad (41)$$

resembling the scaling of rotation peaking observed in discharges with counter-current peaking, and comparable in magnitude for order-unity f_L.[4, 5, 7, 8, 9, 10]

[24] The nonzonal curvature-mediated energy transfer term $\propto \tilde{f}_e^{\rm ev} \mathcal{K}(J_0\tilde{\phi})$ also becomes small for adiabatic electrons, although this is not central to our argument.

[25] The electrostatic energy transfer $T_{\phi i}^{\parallel}$ in this case will be (ZT_{e0}/T_{i0}) times the energy transfer to ion parallel flows due to the parallel density gradient. However, the nonvanishing parallel ion temperature gradient may behave quite differently from the density gradient.

[26] In principle, other physics (such as a spatially varying turbulent density flux) could also excite an axisymmetric but poloidally asymmetric density, leading to an axisymmetric spin-up term in the same way as the GAM damping. However, this seems unlikely to occur, as there is no apparent statistical or energy-flux drive for this mechanism.

[27] Note that this definition of f_L is slightly different than that in Ref. [23], where f_L also includes energy transfer due to the parallel gradient of ion pressure.

5. Discussion

In this section, we will highlight some features of our symmetry-breaking momentum flux, including requirements for a minimal model, possible effects of electromagnetic fluctuations, the role of full-F energy balance, and preliminary comparison with experiment.

Our momentum flux term $\Pi_\varphi^{(2)}$ is independent of toroidal rotation and its radial gradient, thus represents a residual stress. The symmetry-breaking occurs due to the similarity in form between the residual stress term $\Pi_\varphi^{(2)}$ and the free-energy transfer term $T_{\phi i}^{\parallel}$. Fundamentally, $T_{\phi i}^{\parallel}$ has a preferred sign because of steady-state free-energy balance in parameter regimes where strong dissipation acts via the ion parallel flow energy $U_{\delta i}^{\text{od}}$, as demonstrated in Sec. 4.2.[28] In particular, this symmetry breaking follows from free-energy balance for fully saturated turbulence, thus it is a truly nonlinear mechanism. Unlike quasilinear calculations, our model does not rely on any assumed linear phase relationships. Since our momentum flux is driven by a free-energy transfer term, rather than a source term, damped modes (like GAMs) may be as important (or more) as the unstable modes in driving this term. However, our spin-up mechanism may only act in regimes with low-frequency turbulent fluctuations $\omega \lesssim k_\parallel v_{ti}$, since higher-frequency fluctuations do not strongly excite ion parallel flows. One important consequence is that this mechanism is likely weak in the edge region since the steepness of the edge profiles $L_\perp^{\text{edge}} \ll (k_\perp \rho_i / k_\parallel)$ implies that edge turbulence drift frequencies $\sim k_\perp \rho_i v_{ti}/L_\perp^{\text{edge}}$ are much higher than $k_\parallel v_{ti}$, while typical edge q is large enough to prevent effective ion Landau damping of GAMs.

The minimum requirements for a set of equations to model this residual stress mechanism are less stringent than one might expect. Our model is radially local, and does not rely on any profile effects, so a radially local delta-f model is enough. Either linear or nonlinear polarization may be used in general, as long as the conservative structure is not violated, since the relevant linear-polarization simplification is the one made to the energy transfer term, e.g. to discard $(\dot{\boldsymbol{R}} \cdot \nabla H_p)$ relative to $(\dot{\boldsymbol{R}} \cdot \nabla H_1)$ in Eq. (10), almost always a good approximation.[29] Further, even though the momentum flux term results from a higher-order drift that does not affect the leading-order delta-f fluctuations, the statistics of that momentum flux $\Pi_\varphi^{(2)}$ are slaved to the free-energy transfer term $T_{\phi i}^{\parallel}$, which is already well-determined at leading order. In this sense, the momentum flux is 'parasitic': it is determined by leading-order fluctuations, but does not directly feed back on them, although the eventual resulting rotation profile may have an effect. Even so, self-consistent simulations retaining v_{E2}^x remain desirable, in order to verify that the predicted momentum flux is not significantly modified by other effects of the geometrically higher-order portion of the $\boldsymbol{E} \times \boldsymbol{B}$ drift. Critically, the model must respect the relevant conservation laws, specifically free energy conservation for the delta-f equations, since it is the steady-state free-energy balance that drives the symmetry breaking.

How do electromagnetic effects modify our picture? Note first that for a typical low-β plasma, the Alfvén speed is much faster than the ion thermal speed, so electromagnetic fluctuations are generally too high-frequency to excite our residual stress mechanism. They are also fast enough that electron response is not even approximately adiabatic. Further, note that the symmetry-breaking portion of the $\boldsymbol{E} \times \boldsymbol{B}$ drift (v_{E2}^x) follows only from $\nabla_\parallel \phi$, the linear, electrostatic portion of the parallel electric field $E_\parallel$. Although the fluctuating vector potential may contribute to the $\boldsymbol{E} \times \boldsymbol{B}$ drift via fluctuating magnetic direction, magnetic field strength, and inductive electric field, all of these are much smaller than our symmetry-breaking portion, given in Eqs. (33) and (34),[30] thus may be neglected in evaluating $\boldsymbol{v}_E$. However, the inductive parallel electric field $-c^{-1}\partial_t A_\parallel$ may contribute significantly to $E_\parallel$,

[28] In principle, our mechanism could drive co-current rotation peaking for $T_{\phi i}^{\parallel} < 0$, an "inverse Landau damping" regime, as occurs quasilinearly for the slab ITG mode. However, this situation is unlikely to occur in saturated turbulence, due to the absence of any strong free-energy source for $U_{\delta i}^{\text{od}}$ and to the tendency of the electron adiabatic response to drive ion parallel flows.

[29] In either case, one may evaluate the Hamiltonian drifts in this term's $\dot{\boldsymbol{R}}$ as $(c/ZeB_\parallel^*)\hat{\boldsymbol{b}} \times \nabla H_0$, since $\hat{\boldsymbol{b}} \times \nabla(H_1 + H_p) \cdot \nabla(H_1 + H_p) = \hat{\boldsymbol{b}} \times \nabla H_1 \cdot \nabla H_1 = 0$.

[30] Let's estimate contributions of the fluctuating vector potential to v_E^x, compared with our symmetry-breaking portion $v_{E2}^x = (c/B_0) b_y \nabla_\parallel (J_0 \phi) \sim c\tilde{\phi}/B_0 r$. First, fluctuations in the magnetic direction $\tilde{\boldsymbol{b}} = B^{-1}\nabla \times (A_\parallel \hat{\boldsymbol{b}}) = B^{-1}(\nabla A_\parallel) \times \hat{\boldsymbol{b}} + B^{-1} A_\parallel \nabla \times \hat{\boldsymbol{b}}$ are seen to be small:

$$(c/B)\tilde{\boldsymbol{b}}\times\nabla(J_0\phi)\cdot\nabla x = (c/B^2)[(\nabla A_\parallel \times \hat{\boldsymbol{b}}) + A_\parallel(\nabla\times\hat{\boldsymbol{b}})]\cdot\nabla(J_0\phi)\times\nabla x$$

with

$$\frac{\frac{c}{B^2}(\nabla A_\parallel \times \hat{\boldsymbol{b}})\cdot\nabla(J_0\phi)\times\nabla x}{(c/B_0) b_y \nabla_\parallel J_0\phi} = \frac{-(\nabla A_\parallel \cdot \nabla x)\nabla_\parallel J_0\phi}{(B^2/B_0) b_y \nabla_\parallel J_0 \phi} \sim b_p \frac{k_\perp A_\parallel}{B} \ll 1$$

and

$$\frac{\frac{c}{B^2} A_\parallel (\nabla\times\hat{\boldsymbol{b}})\cdot\nabla(J_0\phi)\times\nabla x}{(c/B_0) b_y \nabla_\parallel (J_0\phi)} \sim \frac{A_\parallel R^{-1}(k_\perp \phi)}{B\tilde{\phi}/r} \sim \frac{k_\perp A_\parallel}{B}\frac{r}{R} \ll 1.$$

For the inductive electric field, note that only the perpendicular portion of the perturbed vector potential $\boldsymbol{A}_\perp$ contributes to the $\boldsymbol{E} \times \boldsymbol{B}$ drift. Pressure balance allows us to order the fluctuating field strength $\tilde{B}_\parallel$ by taking $8\pi\tilde{p} \sim (B_0 + \tilde{B}_\parallel)^2 - B_0^2 \approx 2B_0\tilde{B}_\parallel$ for fluctuating plasma pressure $\tilde{p}$, thus $k_\perp A_\perp / B \sim \tilde{B}_\parallel / B \sim 8\pi\tilde{p}/2B^2$. Taking $\partial_t \tilde{p} \sim \boldsymbol{v}_E \cdot \nabla p_0 \sim (c/B_0) k_\perp \tilde{\phi} p_0 / L_\perp$ we may then estimate the relative contribution

$$\frac{\frac{c}{B}\hat{\boldsymbol{b}} \times c^{-1}\partial_t \boldsymbol{A}_\perp}{(c/B_0) b_y \nabla_\parallel (J_0\phi)} \sim \frac{\partial_t 4\pi\tilde{p}/k_\perp B}{c\tilde{\phi}/r} \sim \frac{4\pi p_0}{B^2}\frac{r}{L_\perp} \ll 1,$$

actually cancelling the $-\nabla_\parallel \phi$ term in the ideal MHD regime.[31] Since the energy transfer from fields to $U^{\mathrm{od}}_{\delta i}$ is due to ion parallel current times the total $E_\parallel$, as one may infer e.g. from Eq. (30), the effect of $\partial_t A_\parallel$ will be to decorrelate the net energy transfer to flows from the $\propto f_i^{\mathrm{od}} v_\parallel \nabla_\parallel \phi$ transfer term, which is all that appears in the momentum flux $\Pi^{(2)}_{\varphi i}$. So, rotation peaking due to our mechanism may be expected to be very weak or absent in strongly electromagnetic regimes such as ideal MHD.

Interestingly, a term analogous to $T^{\parallel}_{\phi s}$ appears in the full-F energy balance [Eqs. (9) and (10)], coming from the parallel flow ($v_\parallel \boldsymbol{B}/B^*_\parallel$) part of $\dot{\boldsymbol{R}}$. This shows that the net free-energy transfer from electrons to ions in the ∼adiabatic electron case (Sec. 4.2) is accompanied by a transfer of actual thermal energy from F_e to F_i. In certain regimes with $T_{e0} > T_{i0}$, it is therefore not impossible that full-F thermal energy transfer from electrons to ions could also drive rotation peaking. However, the size of this transfer channel is small: it may be estimated as $\int \mathrm{d}\Lambda\, F_s v_\parallel (\boldsymbol{B}/B^*_\parallel) \cdot \nabla ZeJ_0\phi \sim (\rho_*^2 k_\parallel v_{ti}) n_{e0} T_{e0} V_{\mathrm{pl}} \sim n_{e0} T_{e0} V_{\mathrm{pl}}/\tau_E$ for $\rho_* \doteq (\rho_i/L_\perp) \ll 1$ and gyro-Bohm $\tau_E \sim (L_\perp/\rho_*^2 v_{ti})$, taking profile scale length $L_\perp$ of the same order as $k_\parallel^{-1}$. In contrast, collisional energy transfer should occur at a rate $\sim \nu_{ie} n_{e0}(T_{e0} - T_{i0}) V_{\mathrm{pl}}$ for electron-ion energy-transfer collision rate ν_{ie}. Assuming $\nu_{ie}\tau_E \gg 1$, as is both typical for present-day experiments and required for any eventual fusion reactor, simple electron-ion collisions will dominate the $F_e H_0 \leftrightarrow F_i H_0$ transfer pathway and keep the two species' temperatures similar, at least in the core where the parasitic momentum flux may be active.

Are there other related forms between energy transfer channels and momentum flux terms? While this is not impossible, a careful comparison of the momentum flux terms in Eq. (12) with the energy transfer terms in Eqs. (29)–(32) has not exposed another pair comparable to $\Pi^{(2)}_\varphi$ and $T^{\parallel}_{\phi i}$.[32] For Eqs. (9)–(11), which use nonlinear polarization, the full-F energy transfer term $[-\int \mathrm{d}\Lambda\, F_s v_\parallel (\boldsymbol{B}/B^*_\parallel)\cdot\nabla H_p]$ has a partner term in the momentum flux equation [the geometric correction to $\langle F_s m_s v_\parallel b_\varphi (c/ZeB^*_\parallel)\hat{\boldsymbol{b}} \times \nabla H_p \cdot \nabla V\rangle$]. This pair is analogous to $T^{\parallel}_{\phi i}$ and $\Pi^{(2)}_\varphi$, but is much smaller since $H_p \ll H_1$.

A detailed, quantitative comparison with experiment is well beyond the scope of a simple analytical model as presented here, but we offer a few brief comments. First, the basic scaling [Eqs. (39)–(41), roughly predicting the toroidal velocity at the $q = 1$ surface minus that at pedestal top] exhibits Rice-like scaling $\propto T_0/I_p$ and is of the same order of magnitude as experimental observations of counter-current core rotation peaking [4, 5, 7, 8, 9, 10]. Since our model is a residual stress, it is consistent with peaked intrinsic rotation profiles that pass through zero [4, 5, 6, 7, 8, 9, 10]. The dependence of this model solely on turbulence properties, rather than depending on equilibrium effects like neoclassical flows, allows it to be consistent with the threshhold-like dependence exhibited by core rotation reversals [7, 14, 29]. As one other interesting point of comparison, an extensive database of intrinsic rotation discharges (in L- and H-modes, with various heating methods) showed a robust linear relationship between density peaking and counter-current core rotation peaking [8]. Particle peaking in the core is related to electron drift resonance, which becomes active for $\omega \lesssim k_\perp v_{te}\rho_e/R$ [30, 31], a frequency criterion that is quite similar to that for our counter-current peaking mechanism $\omega \lesssim v_{ti}/qR$, with typically order-unity ratio $(k_\perp v_{te}\rho_e/R)/(v_{ti}/qR) \sim qk_\perp\rho_i(ZT_{e0}/T_{i0})$. This suggests that turbulence regimes that have a lot of low-frequency fluctuations will independently excite both density and counter-current rotation peaking, while those with predominantly higher-frequency turbulent fluctuations will not excite either. More quantitative comparisons will require numerical simulation, while qualitative tests could look for correlations between rotation peaking and turbulent fluctuation regimes, expecting counter-current peaking to occur together with low-frequency electrostatic turbulence.

6. Summary

We identify a portion of the radial $\boldsymbol{E}\times\boldsymbol{B}$ drift, usually neglected in local delta-f formulations, that drives an outward flux of co-current momentum, resulting in counter-current rotation peaking in the tokamak core. This part of the $\boldsymbol{E}\times\boldsymbol{B}$ drift, v^x_{E2}, is smaller than the typically retained portion (v^x_{E1}) by $k_\parallel/(k_\perp b_p)$ but, unlike v^x_{E1}, it is not prohibited from driving residual stress in an up-down symmetric magnetic geometry

assuming a low-β plasma. Modification of the B^{-1} factor is similarly small in β, since

$$\frac{c[(B+\tilde{B}_\parallel)^{-1}-B^{-1}]\hat{\boldsymbol{b}}\times\nabla(J_0\phi)}{(c/B_0)b_y\nabla_\parallel(J_0\phi)} \sim (k_\perp r)\frac{\tilde{B}_\parallel}{B_0} \sim (k_\perp r\frac{\tilde{p}}{p_0})\frac{4\pi p_0}{B^2} \ll 1,$$

where $k_\perp r\tilde{p}/p_0$ is broadly order-unity.

[31] In fact, in a near-ideal-MHD regime, one may estimate that the small surviving $E_\parallel$ will be anticorrelated with $(-\nabla_\parallel\phi)$, which could potentially lead to co-current peaking. However, this effect (if any) would be very weak due to high frequencies and the near-cancellation between $-c^{-1}\partial_t A_\parallel$ and $-\nabla_\parallel\phi$ in $E_\parallel$.

[32] This is easily verified by grouping terms by powers of $v_\parallel$, ϕ, and $A_\parallel$. If you use the flux-divergence form $-\langle F_s \partial_\varphi (H - \frac{Ze}{c} v_\parallel J_0 A_\parallel)\rangle$ from Eq. (12), recall the implicit sum over species, then note that the combinations ZeF_s, $Zev_\parallel F_s$, Zef_s, $Zev_\parallel f_s$ are constrained by the Poisson equation and Ampère's Law, thus behave quite differently from terms with even powers of Z or with factors of m_s. Alternatively, this term can be recast in explicit flux-divergence form, following Ref. [18], removing the near cancellation.

(Secs. 3 and 4.1). Further, $\Pi^{(2)}_{\varphi i}$, the advection of ion parallel toroidal momentum by v^x_{E2}, has an extremely similar form to $T^{\parallel}_{\phi i}$, the term for free-energy transfer from the electrostatic potential energy $U_{\delta E}$ to ion parallel flow energy $U^{\rm od}_{\delta i}$ [Eqs. (36) and (37)]. Since the dominant free energy source supplies energy to $f^{\rm ev}_s$ (the even-in-$v_\parallel$ portion of delta-f_s), while much of the dissipation acts on $f^{\rm od}_s$ (the odd-in-$v_\parallel$ portion of delta-f_s), steady-state free-energy balance implies a net energy transfer from $\sum_s U^{\rm ev}_{\delta s}$ to $\sum_s U^{\rm od}_{\delta s}$. At low frequencies, electron adiabatic response causes much of this transfer to go to $U^{\rm od}_{\delta i}$ via $U_{\delta E}$, resulting in $T^{\parallel}_{\phi i} > 0$ thus $\Pi^{(2)}_{\varphi} \neq 0$ with the sign of B^θ, corresponding to an outflux of co-current toroidal angular momentum (Sec. 4.2). This momentum flux is a residual stress that results from robustly nonlinear symmetry breaking, with no use made of any quasilinear approximations. The use of a free-energy-conserving delta-f model is key to recover this result, but higher-order corrections to the delta-f gyrokinetic equation are not needed. The momentum flux exhibits a scaling and order of magnitude that are consistent with experimental observations [Eqs. (39)–(41)]. The flux becomes small at high frequencies $\omega \gg k_\parallel v_{ti}$, which may explain the experimentally observed correlation between core density and counter-current rotation peaking.

Acknowledgments

Helpful discussions with C. Angioni, G. Hammett, P. Helander, and J. Krommes, and support from the Max-Planck/Princeton Center for Plasma Physics and the U.S. Department of Energy, Office of Science, Contract No. DE-AC02-09CH11466 are gratefully acknowledged.

Appendix A. Derivation using Lagrangian Field Theory

The Lagrangian field theory underlying the gyrokinetic equations used here was first derived in Ref. [24]. In this Appendix, included for completeness, we apply the formalism to a specific Lagrangian to derive the full-F equations given in Sec. 2.1, closely following Ref. [25]. Most symbols are defined in Sec. 2.1. Recall that we use a symplectic formalism here, in which electromagnetic fluctuations ($A_\parallel$) are included in $\boldsymbol{A}^*$ and potential (ϕ) fluctuations in H.

We begin with a single-particle Lagrangian for species s,

$$L_{ps}\left(\boldsymbol{z},\dot{\boldsymbol{z}},t\right) \doteq \frac{Ze}{c}\boldsymbol{A}^*\left(\boldsymbol{z},t\right)\cdot\dot{\boldsymbol{R}}+\mu\frac{m_s c}{Ze}\dot{\vartheta}-H\left(\boldsymbol{z},t\right), \quad \text{(A.1)}$$

where ϑ is the gyroangle. In the definition of L_{ps}, the phase-space coordinates are $\boldsymbol{z} \doteq (\boldsymbol{R}, v_\parallel, \mu, \vartheta)$, with time derivatives $\dot{\boldsymbol{z}} = (\dot{\boldsymbol{R}}, \dot{v}_\parallel, \dot{\mu}, \dot{\vartheta})$ treated as independent variables. Neither $\boldsymbol{A}^*$ nor H depend on $\dot{\boldsymbol{z}}$. The field variables $A_\parallel$ and ϕ, implicit in $\boldsymbol{A}^*$ and H respectively, are evaluated at the gyrocenter position $\boldsymbol{R}$. (The effects of gyroaveraging are explicitly included in the form of L_{ps}.) Consider then phase-space trajectories $\boldsymbol{z}_s(\boldsymbol{z}_{s0}, t)$ and $\dot{\boldsymbol{z}}_s(\boldsymbol{z}_{s0}, t)$ defined over a time interval $t \in [t_0, t_1]$, constrained by $\boldsymbol{z}_s(\boldsymbol{z}_{s0}, t_0) = \boldsymbol{z}_{s0}$. Use D_s to denote the phase-space Jacobian for species s, so that $\int \mathrm{d}^6\boldsymbol{z}\, D_s$ indicates integration over phase space. The system Lagrangian is then defined as

$$L \doteq \sum_s \int \mathrm{d}^6\boldsymbol{z}_{s0} D_{s0}(\boldsymbol{z}_{s0}) F_{s0}(\boldsymbol{z}_{s0}) L_{ps}\left(\boldsymbol{z}_s(\boldsymbol{z}_{s0},t),\dot{\boldsymbol{z}}_s(\boldsymbol{z}_{s0},t),t\right) - \frac{1}{8\pi}\int \mathrm{d}\mathcal{V}\, |\nabla_\perp A_\parallel|^2. \quad \text{(A.2)}$$

We will seek extrema of the corresponding action integral

$$I \doteq \int_{t_0}^{t_1} \mathrm{d}t\, L \quad \text{(A.3)}$$

under variation of the trajectories $\boldsymbol{z}_s(\boldsymbol{z}_{s0}, t)$ and fields $\phi(\boldsymbol{R}, t)$ (in H) and $A_\parallel(\boldsymbol{R}, t)$ (in $\boldsymbol{A}^*$). The endpoints in time and space are held fixed, for both trajectories and fields.

Variation of the trajectories $\boldsymbol{z}_s \to \boldsymbol{z}_s + \delta\boldsymbol{z}_s$ (one s at a time) leads to Euler-Lagrange equations that give the characteristics,[33] which may be written in standard form in terms of L_{ps}:

$$d_t\left(\partial_{\dot{\boldsymbol{z}}_s} L_{ps}\right) = \partial_{\boldsymbol{z}_s} L_{ps}, \quad \text{(A.4)}$$

where d_t is the time derivative along the trajectories, as usual.[34] In Eq. (A.4), the ϑ component yields $\dot{\mu} = 0$,[35] the $v_\parallel$ component yields $\hat{\boldsymbol{b}} \cdot \dot{\boldsymbol{R}} = v_\parallel$,[36] and the $\boldsymbol{R}$ component yields

$$\frac{Ze}{c} d_t \boldsymbol{A}^*\left(\boldsymbol{z}_s\left(t\right), t\right) = \frac{Ze}{c} \partial_{\boldsymbol{R}}|_{\dot{\boldsymbol{R}}}\left(\boldsymbol{A}^* \cdot \dot{\boldsymbol{R}}\right) - \partial_{\boldsymbol{R}} H. \quad \text{(A.5)}$$

Expanding $d_t \to \partial_t + \dot{\boldsymbol{R}} \cdot \partial_{\boldsymbol{R}} + \dot{v}_\parallel \partial_{v_\parallel}$ and using the vector identity $\nabla(\boldsymbol{A}^* \cdot \dot{\boldsymbol{R}}) = \dot{\boldsymbol{R}} \times (\nabla \times \boldsymbol{A}^*) + (\dot{\boldsymbol{R}} \cdot \nabla)\boldsymbol{A}^*$ with $\nabla \doteq \partial_{\boldsymbol{R}}|_{v_\parallel,\mu,\vartheta,\dot{\boldsymbol{z}}}$ here, this may be rewritten as

$$m_s \hat{\boldsymbol{b}} \dot{v}_\parallel - \frac{Ze}{c} \dot{\boldsymbol{R}} \times \boldsymbol{B}^* = -\nabla H - \frac{Ze}{c} \hat{\boldsymbol{b}} \partial_t J_0 A_\parallel. \quad \text{(A.6)}$$

Taking the perpendicular ($\hat{\boldsymbol{b}}\times$) and ~parallel ($\boldsymbol{B}^*\cdot$) components of Eq. (A.6) yields Eqs. (1) and (2). We may also take the μ component to determine $\dot{\vartheta}$,

[33] Note that $D_{s0}(\boldsymbol{z}_{s0})$, $F_{s0}(\boldsymbol{z}_{s0})$, and the field term $-\int \mathrm{d}\mathcal{V}\, |\nabla_\perp A_\parallel|^2/8\pi$ are all independent of the trajectories $\boldsymbol{z}_s$.

[34] As one does the variation of L considering L_{ps} to depend on $\boldsymbol{z}_{s0}$ and t, one may identify $d_t = \partial_t|_{\boldsymbol{z}_{s0}}$.

[35] This follows since H and $\boldsymbol{A}^*$ are both independent of ϑ.

[36] Here we used the fact that $(H - m_s v_\parallel^2/2)$ and J_0 are both independent of $v_\parallel$, in this symplectic formulation.

but this is unnecessary since all other equations are independent of ϑ and $\dot{\vartheta}$.[37]

The distribution function F_s is mapped to Eulerian coordinates by the conservation of phase-space trajectories:

$$D_s(\boldsymbol{z},t)F_s(\boldsymbol{z},t)=\int \mathrm{d}^6\boldsymbol{z}_{s0}\,D_{s0}(\boldsymbol{z}_{s0})F_{s0}(\boldsymbol{z}_{s0})\delta^6\left(\boldsymbol{z}-\boldsymbol{z}_s(\boldsymbol{z}_{s0},t)\right),\quad \text{(A.7)}$$

with time partial[38]

$$\begin{aligned}\partial_t(D_sF_s)&=\int \mathrm{d}^6\boldsymbol{z}_{s0}\,D_{s0}(\boldsymbol{z}_{s0})F_{s0}(\boldsymbol{z}_{s0})(-\dot{\boldsymbol{z}}_s\cdot\partial_{\boldsymbol{z}})\delta^6(\boldsymbol{z}-\boldsymbol{z}_s(\boldsymbol{z}_{s0},t))\\ &=-\partial_{\boldsymbol{z}}\cdot\left[\int \mathrm{d}^6\boldsymbol{z}_{s0}\,D_{s0}(\boldsymbol{z}_{s0})F_{s0}(\boldsymbol{z}_{s0})\dot{\boldsymbol{z}}_s(\boldsymbol{z}_s,t)\delta^6\left(\boldsymbol{z}-\boldsymbol{z}_s(\boldsymbol{z}_{s0},t)\right)\right]\\ &=-\partial_{\boldsymbol{z}}\cdot\left[D_s(\boldsymbol{z},t)\,F_s(\boldsymbol{z},t)\,\dot{\boldsymbol{z}}(\boldsymbol{z},t)\right].\end{aligned}\quad \text{(A.8)}$$

Noting that the velocity-space Jacobian is $2\pi B_\parallel^*/m_s$, Eq. (A.8) is equivalent to Eq. (3).[39]

Finally, we must solve for the fields. Varying the function $\phi\to\phi+\delta\phi$ in I yields the Poisson equation[40]

$$0=\sum_s\int\frac{\mathrm{d}\mathcal{W}}{B_\parallel^*}\Big[ZeJ_0^\dagger(B_\parallel^*F_s)+J_0^\dagger(B_\parallel^*\mathcal{M}J_0\phi)-\phi J_0^\dagger(B_\parallel^*\mathcal{M})\Big],\quad \text{(A.9)}$$

where $\mathcal{M}$ is defined in Eq. (7) and $J_0^\dagger$ is the adjoint to J_0 under spatial integration $\int \mathrm{d}\mathcal{V}$. Similarly, varying $A_\parallel\to A_\parallel+\delta A_\parallel$ in I yields the gyrokinetic Ampère's Law

$$\nabla_\perp^2A_\parallel=-\frac{4\pi}{c}\sum_s\int\frac{\mathrm{d}\mathcal{W}}{B_\parallel^*}ZeJ_0^\dagger\left(B_\parallel^*v_\parallel F_s\right).\quad \text{(A.10)}$$

If we assume J_0 to be self-adjoint under $\int \mathrm{d}\mathcal{V}$, then Eqs. (A.9) and (A.10) reduce to Eqs. (6) and (8). Note that the energy and toroidal angular momentum are also conserved in a more general system with $J_0^\dagger\neq J_0$, as long as Eqs. (A.9) and (A.10) are used instead of Eqs. (6) and (8).

A conservative system with linearized polarization may also be derived via the above procedure, if one simplifies the Hamiltonian to H_0+H_1 and adds a field term $-\sum_s\int \mathrm{d}^6\boldsymbol{z}\,D_{sM}(\boldsymbol{z})F_{sM}(\boldsymbol{z})H_p(\boldsymbol{z},t)$ to the system Lagrangian L. [In the field term, F_{sM} is a static background distribution function, typically taken to be Maxwellian, and D_{sM} is a static background Jacobian (neglecting $A_\parallel$), thus with velocity-space portion simplified to a multiple of $B_{\parallel M}^*\doteq\hat{\boldsymbol{b}}\cdot\nabla\times(\boldsymbol{A}+\frac{c}{Ze}m_sv_\parallel\hat{\boldsymbol{b}})$. Although the field term does not involve the phase-space trajectories $\boldsymbol{z}_s(\boldsymbol{z}_{s0},t)$, thus knows nothing about the time-dependent F_s, it retains information about $\phi(\boldsymbol{R},t)$ via the time- (but not trajectory-) dependent $H_p(\boldsymbol{z},t)$.] Varying the simplified system, one finds that the characteristics [Eqs. (1) and (2)], gyrokinetic equation [Eq. (3) or (5)], and Ampère's Law [Eq. (8) or (A.10)] are unchanged, except for the simplified H. Varying the modified I with respect to ϕ produces a Poisson equation identical to Eq. (A.9), except for the substitution $\mathcal{M}\to\mathcal{M}_M$ with

$$\mathcal{M}_M\doteq-\frac{Z^2e^2}{BB_\parallel^*}\partial_\mu\left(B_{\parallel M}^*F_{sM}\right).\quad \text{(A.11)}$$

Commonly used simplifications of $\mathcal{M}_M$ are given in Ref. [25], but are not needed for the present work.

Appendix B. Toroidal Angular Momentum Conservation

In this Appendix, we demonstrate that the gyrokinetic system given by Eqs. (1)–(3) and (6)–(8) conserves toroidal angular momentum, working directly from the referenced equations themselves. The derivation proceeds in two steps, roughly following Ref. [18]. First, we calculate the evolution of the canonical toroidal angular momentum $\mathcal{P}_\varphi\doteq\frac{Ze}{c}A_\varphi+(\frac{Ze}{c}J_0A_\parallel+m_sv_\parallel)b_\varphi=\frac{Ze}{c}A_\varphi^*$ along the trajectories given by Eqs. (1) and (2). Second, we use quasineutrality to eliminate the contribution of the equilibrium vector potential $\boldsymbol{A}$ from the conserved toroidal angular momentum. We use a standard axisymmetric field formulation $\boldsymbol{B}=B_\varphi\nabla\varphi+\nabla A_\varphi\times\nabla\varphi$, with simple toroidal angle φ,[41] $B_\varphi=\boldsymbol{B}\cdot R^2\nabla\varphi$, and $A_\varphi=\boldsymbol{A}\cdot R^2\nabla\varphi$. We may decompose any arbitrary vector as $\boldsymbol{w}=w_\varphi\nabla\varphi+\boldsymbol{w}_p$ with $w_\varphi=\boldsymbol{w}\cdot R^2\nabla\varphi$ and $\boldsymbol{w}_p\cdot\nabla\varphi=0$, in terms of which $\nabla\times\boldsymbol{w}=\nabla w_\varphi\times\nabla\varphi+\nabla\times\boldsymbol{w}_p$ and $(\nabla\times\boldsymbol{w}_p)_p=\nabla\varphi\times\partial_\varphi\boldsymbol{w}_p$, where $\partial_\varphi\doteq[(R^2\nabla\varphi)\cdot\nabla]$. We also use the relation $\langle\nabla\cdot\boldsymbol{w}\rangle=\partial_V\langle\boldsymbol{w}\cdot\nabla V\rangle$ for the flux-surface average of a divergence.[26]

As our first step, we evaluate $d_t\mathcal{P}_\varphi\doteq\partial_t\mathcal{P}_\varphi+\dot{\boldsymbol{R}}\cdot\nabla\mathcal{P}_\varphi+\dot{v}_\parallel\partial_{v_\parallel}\mathcal{P}_\varphi$ along the characteristics given by Eqs. (1) and (2):

$$B_\parallel^*d_t\mathcal{P}_\varphi=(\nabla A_\varphi^*\times\hat{\boldsymbol{b}}-b_\varphi\boldsymbol{B}^*)\cdot\nabla H+\frac{Ze}{c}v_\parallel\boldsymbol{B}^*\cdot\nabla A_\varphi^*.\quad \text{(B.1)}$$

Decomposing $\boldsymbol{A}^*=A_\varphi^*\nabla\varphi+\boldsymbol{A}_p^*$ and $\hat{\boldsymbol{b}}=b_\varphi\nabla\varphi+\hat{\boldsymbol{b}}_p$, for which $(\partial_\varphi\boldsymbol{A}_p^*)_p=\hat{\boldsymbol{b}}_p\partial_\varphi(J_0A_\parallel)$, shows that $\nabla A_\varphi^*\times\hat{\boldsymbol{b}}-b_\varphi\boldsymbol{B}^*=\nabla A_\varphi^*\times\hat{\boldsymbol{b}}_p-b_\varphi\nabla\times\boldsymbol{A}_p^*$, $(\nabla A_\varphi^*\times\hat{\boldsymbol{b}}-b_\varphi\boldsymbol{B}^*)\cdot\nabla\varphi=-B_\parallel^*$, $(\nabla A_\varphi^*\times\hat{\boldsymbol{b}}_p-b_\varphi\nabla\times\boldsymbol{A}_p^*)_p=0$, $\boldsymbol{B}^*\cdot\nabla A_\varphi^*=$

[37] Since $\dot{\vartheta}$ and D_s are independent of ϑ, if we assume F_{s0} is also independent of ϑ, then so is F_s at all t. Alternatively we may consider the "ring average" $\frac{1}{2\pi}\int \mathrm{d}\vartheta\,F_s$, which is independent of ϑ for any F_{s0} and which supplies all the needed information for the other equations [Eqs. (1), (2), and ring-averaged Eqs. (A.8), (A.9), and (A.10)].

[38] Note that $\boldsymbol{z}_s$ and $\dot{\boldsymbol{z}}_s$ are functions of $\boldsymbol{z}_{s0}$ and t alone. In particular, both $\boldsymbol{z}_s$ and $\dot{\boldsymbol{z}}_s$ are independent of $\boldsymbol{z}$.

[39] The real-space Jacobian is independent of t and $v_\parallel$, and is implicit in the divergence operator $\nabla\cdot$.

[40] The extremization is conceptually clearest if one takes $\phi\to\phi+\alpha\eta$ for real number α and function $\eta(\boldsymbol{R},t)$, then sets $\partial_\alpha I=0$ at $\alpha=0$, for arbitrary η. It is convenient to multiply the integrand in I by $1=\int \mathrm{d}^6\boldsymbol{z}\,\delta^6(\boldsymbol{z}-\boldsymbol{z}_s(\boldsymbol{z}_{s0},t))$. The boundary term at $\mu=0$ vanishes because $J_0(\mu=0)$ is the identity operator.

[41] I use the right-handed (R,z,φ) sign convention, so $\nabla\varphi$ is directed oppositely to the gradient of the azimuthal angle for simple cylindrical coordinates.

$(\nabla \times \boldsymbol{A}_p^*) \cdot \nabla A_\varphi^*$, and $(\nabla \times \boldsymbol{A}_p^*)_p \cdot \nabla A_\varphi^* = (\hat{\boldsymbol{b}}_p \cdot \boldsymbol{B}^*)\partial_\varphi(J_0 A_\parallel)$. Using these results, we may rewrite Eq. (B.1) in the simpler form

$$d_t \mathcal{P}_\varphi = -\partial_\varphi \left[H - (Ze/c)v_\parallel J_0 A_\parallel\right]. \tag{B.2}$$

As our second step, we take appropriate moments of the distribution function, so that we may use quasineutrality [Eq. (6)] to replace the nearly-canceling species-summed $(Ze/c)A_\varphi$ contribution with the $\boldsymbol{E}\times\boldsymbol{B}$ portion of the toroidal angular momentum. First we evaluate the evolution of parallel physical momentum of species s, multiplying Eq. (3) by $b_\varphi m_s v_\parallel / B_\parallel^*$ and flux-surface averaging, recalling that $\int \mathrm{d}\mathcal{W}/B_\parallel^*$ commutes with ∂_t and spatial differentiation and annihilates $\partial_{v_\parallel}$, obtaining

$$\partial_t \langle F_s m_s v_\parallel b_\varphi\rangle + \partial_V \langle F_s m_s v_\parallel b_\varphi \dot{\boldsymbol{R}}\cdot\nabla V\rangle = \langle F_s d_t(m_s v_\parallel b_\varphi)\rangle. \tag{B.3}$$

We may similarly evolve the contribution due to electromagnetic fluctuations (times c/e), multiplying Eq. (3) by $Zb_\varphi(J_0 A_\parallel)/B_\parallel^*$ and flux-surface averaging to get

$$\partial_t \langle F_s b_\varphi Z J_0 A_\parallel\rangle + \partial_V \left\langle F_s b_\varphi Z(J_0 A_\parallel)\dot{\boldsymbol{R}}\cdot\nabla V\right\rangle = \left\langle F_s d_t(Z b_\varphi J_0 A_\parallel)\right\rangle. \tag{B.4}$$

The $\boldsymbol{E}\times\boldsymbol{B}$ contribution is a little more involved. First, we define the polarization $\boldsymbol{P}$ as a solution to[42]

$$\nabla \cdot \boldsymbol{P} \doteq \sum_s Ze \int \mathrm{d}\mathcal{W}\, F_s. \tag{B.5}$$

We time-differentiate Eq. (B.5), substitute using Eq. (3) for each species s, and flux-surface average, obtaining

$$\partial_V \partial_t \langle \boldsymbol{P}\cdot\nabla V\rangle = -\partial_V \left\langle ZeF_s \dot{\boldsymbol{R}}\cdot\nabla V\right\rangle. \tag{B.6}$$

For well-behaved (finite) $\boldsymbol{P}$ and $ZeF_s\dot{\boldsymbol{R}}$, the quantities $(\boldsymbol{P}\cdot\nabla V)$ and $ZeF_s\dot{\boldsymbol{R}}\cdot\nabla V$ must vanish at the magnetic axis ($V=0$), because ∇V goes to zero there. We may therefore integrate Eq. (B.6) in V to obtain

$$\partial_t \langle \boldsymbol{P}\cdot\nabla V\rangle = -\left\langle ZeF_s\dot{\boldsymbol{R}}\cdot\nabla V\right\rangle. \tag{B.7}$$

Since Eq. (6) may be used to relate $\nabla\cdot\boldsymbol{P}$ with the polarization charge, Eq. (B.7) simply states that the net radial current out of any flux-surface-enclosed volume must vanish. Now multiply Eq. (B.7) by the flux function $-\frac{1}{c}\partial_V A_\varphi$ to obtain

$$-\partial_t \frac{1}{c}\langle \boldsymbol{P}\cdot\nabla A_\varphi\rangle = \frac{1}{c}\langle ZeF_s\dot{\boldsymbol{R}}\cdot\nabla A_\varphi\rangle = \langle F_s d_t(ZeA_\varphi/c)\rangle. \tag{B.8}$$

The quantity $-\frac{1}{c}\langle \boldsymbol{P}\cdot\nabla A_\varphi\rangle$ is a generalized expression for the toroidal angular momentum in the $\boldsymbol{E}\times\boldsymbol{B}$ motion, as has been demonstrated using the quasineutrality relation [18]. Finally, summing Eqs. (B.3), (B.4) times (e/c), and (B.8), then simplifying with Eq. (B.2), we obtain the desired evolution equation for the toroidal angular momentum:

$$\begin{aligned}\partial_t\langle F_s[m_s v_\parallel + (Ze/c)J_0 A_\parallel]b_\varphi\rangle - \partial_t\langle \boldsymbol{P}\cdot\nabla A_\varphi\rangle/c \\ + \partial_V\left\langle F_s[m_s v_\parallel + (Ze/c)J_0A_\parallel]b_\varphi\dot{\boldsymbol{R}}\cdot\nabla V\right\rangle \\ = \langle F_s d_t\mathcal{P}_\varphi\rangle = -\left\langle F_s\partial_\varphi[H-(Ze/c)v_\parallel J_0 A_\parallel]\right\rangle.\end{aligned} \tag{B.9}$$

This equation is the toroidal momentum transport equation for our gyrokinetic model, the symplectic-form analog of Ref. [18]'s Eq. (80).

The terms on the LHS of Eq. (B.9) respectively capture the time variation of parallel toroidal angular momentum and of $\boldsymbol{E}\times\boldsymbol{B}$ toroidal angular momentum as well as the divergence of the radial flux of parallel toroidal angular momentum. Although it may not be immediately obvious, the RHS captures the divergence of the radial flux of $\boldsymbol{E}\times\boldsymbol{B}$ toroidal angular momentum. This is shown for various functional forms of H in Ref. [18], albeit in a canonical formulation (with $A_\parallel$ in the Hamiltonian H, rather than in $\boldsymbol{A}^*$ as here). For our purposes, it is adequate to demonstrate that the RHS of Eq. (B.9) is the divergence of *some* radial flux term, without evaluating an explicit form for that flux.

Consider first the Hamiltonian contribution. Since the zeroth-order Hamiltonian is axisymmetric ($\partial_\varphi H_0 = 0$), we only need to treat H_1 and H_p. Using the facts that J_0 is both axisymmetric (so $\partial_\varphi J_0 = J_0\partial_\varphi$) and self-adjoint under $\int \mathrm{d}\mathcal{V}$,[43] that the magnetic geometry is axisymmetric, and that $\int \mathrm{d}\mathcal{W}/B_\parallel^*$ commutes with real-space differentiation and integration and annihilates velocity-space derivatives,[44] we may integrate the term radially (over all V) to find

$$\begin{aligned}\int \mathrm{d}V\,\langle F_s\partial_\varphi H\rangle = \sum_s\int \mathrm{d}\Lambda\, F_s\partial_\varphi H = \int \mathrm{d}\mathcal{V}(\partial_\varphi\phi) \\ \times\sum_s\int\frac{\mathrm{d}\mathcal{W}}{B_\parallel^*}\left[ZeJ_0(B_\parallel^*F_s) + J_0(B_\parallel^*\mathcal{M}J_0\phi) - \phi J_0(B_\parallel^*\mathcal{M})\right] \\ = 0,\end{aligned} \tag{B.10}$$

where the last form vanished due to quasineutrality [Eq. (6)]. Since $\int \mathrm{d}V\langle F_s\partial_\varphi H\rangle = 0$, we may express the contribution of $\langle F_s\partial_\varphi H\rangle$ as the divergence of some radial flux that vanishes at the boundary. Ref. [18] gives explicit forms of this flux for various forms of H.

Consider now the electromagnetic term. Using Eq. (8) and the facts that J_0 is Hermitian under $\int \mathrm{d}\mathcal{V}$

[42] Eq. (B.5) only defines $\boldsymbol{P}$ up to an arbitrary curl. However, the arbitrary divergence-free portion makes no contribution to Eq. (B.6), (B.8), (B.9), or (12). [If we let $\mathrm{d}\boldsymbol{S}$ be the outward area differential for flux surface V, then for arbitrary vector $\boldsymbol{w}$ we have $\int_V \mathrm{d}\mathcal{V}\,\nabla\times\boldsymbol{w}\cdot\nabla V = \int_V \mathrm{d}\mathcal{V}\,\nabla\cdot(\boldsymbol{w}\times\nabla V) = \int \mathrm{d}\boldsymbol{S}\cdot\boldsymbol{w}\times\nabla V = 0$, since $\mathrm{d}\boldsymbol{S}\parallel\nabla V$.]

[43] In fact, as discussed in Appendix A, we do not need to make the typical assumption that J_0 is self-adjoint. However, if we allow non-self-adjoint J_0, then we must use the general quasineutrality relation [Eq. (A.9)] rather than the simplified one [Eq. (6)].

[44] In the integration by parts on μ, the boundary term at $\mu = 0$ vanishes because $J_0(\mu = 0)$ is the identity operator.

and commutes with ∂_φ, we obtain[45]

$$\int \mathrm{d}V \langle F_s \partial_\varphi (Zev_\parallel J_0 A_\parallel / c)\rangle = \frac{1}{c}\sum_s \int \mathrm{d}\Lambda\, ZeF_s v_\parallel J_0 \partial_\varphi A_\parallel$$

$$= \frac{1}{4\pi}\int \mathrm{d}\mathcal{V}\,(\partial_\varphi A_\parallel)\frac{4\pi}{c}\sum_s \int \frac{\mathrm{d}\mathcal{W}}{B_\parallel^*} ZeJ_0(B_\parallel^* F_s v_\parallel)$$

$$= -\int \frac{\mathrm{d}\mathcal{V}}{4\pi}(\partial_\varphi A_\parallel)\nabla_\perp^2 A_\parallel = -\int \frac{\mathrm{d}\mathcal{V}}{4\pi}\nabla\cdot[(\partial_\varphi A_\parallel)\nabla_\perp A_\parallel]. \quad \text{(B.11)}$$

We may therefore express $\langle F_s \partial_\varphi (\frac{Ze}{c} v_\parallel J_0 A_\parallel)\rangle$ as the divergence of the flux in the last term of Eq. (B.11) (an expression for the Maxwell stress), plus the divergence of some other radial flux that vanishes at the boundary.

At the end of Appendix A, we described how one may derive a full-F gyrokinetic system with linearized polarization, equivalent to Eqs. (1)–(3), (6), and (8) with the simplifications $H \to (H_0 + H_1)$ and $\mathcal{M} \to \mathcal{M}_M$. As is easily verified, the derivations of Eqs. (B.2) and (B.9) are unchanged by these simplifications, so that Eqs. (B.2) and (B.9) also hold for the system with linearized polarization, as long as they are interpreted using the simplified Hamiltonian $(H_0 + H_1)$ and the linearized polarizability $\mathcal{M}_M$. The demonstration that the RHS of Eq. (B.9) is conservative is slightly modified by the simplifications $H \to (H_0 + H_1)$ and $\mathcal{M} \to \mathcal{M}_M$. In particular, although Eq. (B.11) is not changed by linearized polarization, Eq. (B.10) is modified to

$$\int \mathrm{d}V \langle F_s \partial_\varphi H\rangle = \sum_s \int \mathrm{d}\Lambda\, F_s \partial_\varphi (ZeJ_0\phi)$$

$$= \int \mathrm{d}\mathcal{V}(\partial_\varphi \phi)\sum_s \int \frac{\mathrm{d}\mathcal{W}}{B_\parallel^*} ZeJ_0(B_\parallel^* F_s)$$

$$= -\int \mathrm{d}\mathcal{V}(\partial_\varphi \phi)\sum_s \int \frac{\mathrm{d}\mathcal{W}}{B_\parallel^*}[J_0(B_\parallel^* \mathcal{M}_M J_0\phi) - \phi J_0(B_\parallel^* \mathcal{M}_M)]$$

$$= -\frac{1}{2}\sum_s \int \frac{\mathrm{d}\mathcal{W}}{B_\parallel^*}\int \mathrm{d}\mathcal{V}\, B_\parallel^* \mathcal{M}_M \partial_\varphi [(J_0\phi)^2 - J_0(\phi^2)] = 0, \quad \text{(B.12)}$$

where the last equality follows because $(B_\parallel^* \mathcal{M}_M)$ is axisymmetric.

References

[1] J. S. deGrassie, Plasma Phys. Controlled Fusion **51**, 124047 (2009).

[2] E. Strait, T. S. Taylor, A. D. Turnbull, J. R. Ferron, L. L. Lao, B. Rice, O. Sauter, S. J. Thompson, and D. Wróblewski, Phys. Rev. Lett. **74**, 2483 (1995).

[3] E. J. Doyle *et al.*, Nucl. Fusion **47**, S18 (2007).

[4] J. S. deGrassie, J. E. Rice, K. H. Burrell, R. J. Groebner, and W. M. Solomon, Phys. Plasmas **14**, 056115 (2007).

[45] Here we also use $2\int \mathrm{d}\mathcal{V}\,(\nabla_\perp A_\parallel)\cdot(\nabla_\perp \partial_\varphi A_\parallel) = \int \mathrm{d}\mathcal{V}\,\partial_\varphi |\nabla_\perp A_\parallel|^2 = 0$.

[5] L.-G. Eriksson, T. Hellsten, M. F. F. Nave, J. Brzozowski, K. Holmström, T. Johnson, J. Ongena, K.-D. Zastrow, and JET-EFDA Contributors, Plasma Phys. Controlled Fusion **51**, 044008 (2009).

[6] O. Sauter, B. P. Duval, L. Federspiel, F. Felici, T. P. Goodman, A. Karpushov, S. Puddu, J. Rossel, and the TCV team, in *Fusion Energy Conference 2010 Book of Abstracts* (IAEA, 2010) p. 180.

[7] J. E. Rice *et al.*, Nucl. Fusion **51**, 083005 (2011).

[8] C. Angioni *et al.*, Phys. Rev. Lett. **107**, 215003 (2011).

[9] R. M. McDermott *et al.*, Plasma Phys. Controlled Fusion **53**, 124013 (2011).

[10] T. Stoltzfus-Dueck, A. N. Karpushov, O. Sauter, B. P. Duval, B. Labit, H. Reimerdes, W. A. J. Vijvers, Y. Camenen, and the TCV Team, Phys. Plasmas **22**, 056118 (2015).

[11] T. Stoltzfus-Dueck, Phys. Rev. Lett. **108**, 065002 (2012).

[12] T. Stoltzfus-Dueck, Phys. Plasmas **19**, 055908 (2012).

[13] T. Stoltzfus-Dueck, A. N. Karpushov, O. Sauter, B. P. Duval, B. Labit, H. Reimerdes, W. A. J. Vijvers, Y. Camenen, and the TCV Team, Phys. Rev. Lett. **114**, 245001 (2015).

[14] A. Bortolon, B. P. Duval, A. Pochelon, and A. Scarabosio, Phys. Rev. Lett. **97**, 235003 (2006).

[15] J. E. Rice *et al.*, Nucl. Fusion **53**, 033004 (2013).

[16] A. G. Peeters *et al.*, Nucl. Fusion **51**, 094027 (2011).

[17] J.-K. Park *et al.*, Phys. Rev. Lett. **111**, 095002 (2013).

[18] B. Scott and J. Smirnov, Phys. Plasmas **17**, 112302 (2010).

[19] A. J. Brizard and N. Tronko, Phys. Plasmas **18**, 082307 (2011).

[20] S. D. Scott *et al.*, Phys. Rev. Lett. **64**, 531 (1990).

[21] T. S. Hahm, P. H. Diamond, O. D. Gurcan, and G. Rewoldt, Phys. Plasmas **14**, 072302 (2007).

[22] A. G. Peeters, C. Angioni, Y. Camenen, F. J. Casson, W. A. Hornsby, A. P. Snodin, and D. Strintzi, Phys. Plasmas **16**, 062311 (2009).

[23] T. Stoltzfus-Dueck submitted to *Phys. Plasmas.*

[24] H. Sugama, Phys. Plasmas **7**, 466 (2000).

[25] B. Scott, Phys. Plasmas **17**, 102306 (2010).

[26] W. D. D'haeseleer, W. N. G. Hitchon, J. D. Callen, and J. L. Shohet, *Flux Coordinates and Magnetic Field Structure: A Guide to a Fundamental Tool of Plasma Theory* (Springer-Verlag, 1991).

[27] S. Hamada, Nucl. Fusion **2**, 23 (1962).

[28] B. Scott, Phys. Plasmas **5**, 2334 (1998).

[29] J. E. Rice *et al.*, Phys. Rev. Lett. **107**, 265001 (2011).

[30] C. Angioni, Y. Camenen, F. J. Casson, E. Fable, R. M. McDermott, A. G. Peeters, and J. E. Rice, Nucl. Fusion **52**, 114003 (2012).

[31] E. Fable, C. Angioni, and O. Sauter, Plasma Phys. Controlled Fusion **52**, 015007 (2010).

P.O. Box 451, Princeton, NJ 08543
Phone: 609-243-2245
Fax: 609-243-2751

E-mail: publications@pppl.gov

Website: http://www.pppl.gov